Journal of Hazardous Materials 474 (2024) 134763

Contents lists available at ScienceDirect

Journal of Hazardous Materials

journal homepage: www.elsevier.com/locate/jhazmat

Research Paper

Sources of acellular oxidative potential of water-soluble fine ambient particulate matter in the midwestern United States

Haoran Yu [a,d], Yixiang Wang [b,d], Joseph V. Puthussery [c,d], Vishal Verma [d,*]

[a] Department of Civil and Environmental Engineering, University of Alberta, 9211 116th St, Edmonton, AB T6G 1H9, Canada
[b] College of Health, Lehigh University, 124 E Morton St, Bethlehem, PA 18015, United States
[c] Department of Energy, Environmental & Chemical Engineering, Washington University in St. Louis, 1 Brookings Drive, St. Louis, MO 63130-4899, United States
[d] Department of Civil and Environmental Engineering, University of Illinois at Urbana-Champaign, 205 North Mathews Avenue, Urbana, IL 61801, United States

HIGHLIGHTS

- Emission sources in the Midwest US contribute disproportionately to $PM_{2.5}$ mass vs. oxidative potential of $PM_{2.5}$.
- Secondary sources, coal combustion, biomass burning, and primary vehicular emissions dominated $PM_{2.5}$ mass.
- Local sources (industrial, parking, and agricultural emissions) contribute minorly to $PM_{2.5}$ mass but substantially to OP.
- Organic carbon and transition metals (e.g., Cu, Fe, and Mn) showed moderate-to-strong correlation with OP.

GRAPHICAL ABSTRACT

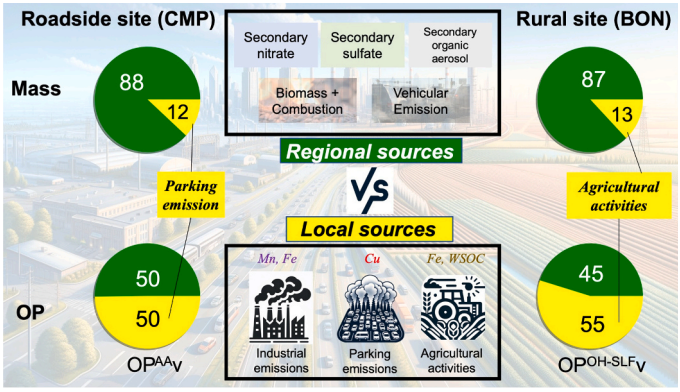

ARTICLE INFO

Keywords:
Oxidative potential
$PM_{2.5}$ chemical composition
Source apportionment
Health
Effects
Positive matrix factorization

ABSTRACT

Ambient fine particulate matter ($PM_{2.5}$) is associated with numerous health complications, yet the specific $PM_{2.5}$ chemical components and their emission sources contributing to these health outcomes are understudied. Our study analyzes the chemical composition of $PM_{2.5}$ collected from five distinct locations at urban, roadside and rural environments in midwestern region of the United States, and associates them with five acellular oxidative potential (OP) endpoints of water-soluble $PM_{2.5}$. Redox-active metals (i.e., Cu, Fe, and Mn) and carbonaceous species were correlated with most OP endpoints, suggesting their significant role in OP. We conducted a source apportionment analysis using positive matrix factorization (PMF) and found a strong disparity in the contribution of various emission sources to $PM_{2.5}$ mass vs. OP. Regional secondary sources and combustion-related aerosols contributed significantly (> 75 % in total) to $PM_{2.5}$ mass, but showed weaker contribution (43–69 %) to OP. Local sources such as parking emissions, industrial emissions, and agricultural activities, though accounting marginally to $PM_{2.5}$ mass (< 10 % for each), significantly contributed to various OP endpoints (10–50 %). Our results demonstrate that the sources contributing to $PM_{2.5}$ mass and health effects are not necessarily same, emphasizing the need for an improved air quality management strategy utilizing more health-relevant $PM_{2.5}$ indicators.

* Corresponding author.
E-mail address: vverma@illinois.edu (V. Verma).

https://doi.org/10.1016/j.jhazmat.2024.134763
Received 25 March 2024; Received in revised form 22 May 2024; Accepted 28 May 2024
Available online 29 May 2024
0304-3894/© 2024 The Authors. Published by Elsevier B.V. This is an open access article under the CC BY license (http://creativecommons.org/licenses/by/4.0/).

1. Introduction

Ambient fine particulate matter (particles with aerodynamic diameter less than 2.5 μm, $PM_{2.5}$) has been recognized as a key air pollutant that poses a serious threat to human health. Numerous studies have reported its association with various health outcomes, such as cardiovascular-related morbidity and mortality [1-4], respiratory [5-7] and neurodegenerative diseases [8-10], low birth weight [11-13], and risk of diabetes [14-16]. Consequently, World Health Organization (WHO) Air Quality Guidelines (AQG) suggest using mass concentration of ambient $PM_{2.5}$ as an air quality index for regulation [17]. However, the rationale of using $PM_{2.5}$ mass as a health metric has always been debated due to the complex and variable chemical composition of ambient $PM_{2.5}$. Mostofsky et al. [18] reported significant associations between several trace elements in ambient $PM_{2.5}$, including Fe, Ni, and V, and risk of stroke in patients with cardiovascular diseases in Boston, MA, suggesting the likelihood of much higher toxicity of these components carrying little mass. Bell et al. [19] found strong correlations between cardiovascular hospital visits for the Medicare population (i.e., people more than 65 years of age) and ambient concentrations of Ca, V, and Zn. The same study also reported significant associations between respiratory disease related hospital admissions and certain trace elements (Al, Ca, Ni, Ti, and V). These and several other studies [20-23] indicate that the health impacts of $PM_{2.5}$ could be driven by only a small fraction of its mass, questioning the relevance and effectiveness of regulating total $PM_{2.5}$ mass.

Since ambient $PM_{2.5}$ originates from heterogeneous sources, its chemical composition is highly uncertain and variable in space and time. Therefore, it is impractical to identify and measure all toxic components, which highlights the need to derive a biologically-relevant property of ambient $PM_{2.5}$ that could better represent the health outcomes of $PM_{2.5}$. In recent decades, the oxidative potential (OP) of $PM_{2.5}$, which is defined as the capability of $PM_{2.5}$ to catalyze the depletion of antioxidants and the generation of reactive oxygen species (ROS) in human body, has been proposed as a potentially health-relevant metric. Numerous evidences show a stronger association of OP with multiple health outcomes, including cardiorespiratory emergency room visits [24-27], asthma symptoms [28,29], respiratory hospitalizations in children [30], increased fractional exhaled nitric oxide (FeNO) [31-33], and diabetes prevalence [34,35], in comparison to $PM_{2.5}$ mass. In more inclusive terms, OP can be expressed with different endpoints, such as the consumption rate of ascorbic acid (AA; OP^{AA}), glutathione (GSH; OP^{GSH}), dithiothreitol (DTT; OP^{DTT}), the production rate of hydroxyl radical (•OH) in surrogate lung fluid (SLF) or DTT ($OP^{OH\text{-}SLF}$ and $OP^{OH\text{-}DTT}$, respectively), and the cellular generation of ROS (macrophage ROS) [28,36]. However, multiple studies have reported different spatiotemporal patterns [37,38] and different set of chemical species driving the response of these assays [37,39]. Moreover, recent studies investigating their spatiotemporal patterns have shown weak correlations among these OP endpoints [39,40]. Our previous study, Yu et al. [40], reported an overall poor-to-moderate correlations among five commonly used OP endpoints in the Midwestern US, indicating that these endpoints potentially represent distinct biological pathways. Hence, it is crucial to assess multiple endpoints for a comprehensive OP analysis.

Although several metropolitan areas in the Midwestern US, such as Indianapolis, Chicago, St. Louis, and Detroit, are generally recognized as highly air polluted districts [41-44], a comprehensive investigation on the sources of ambient $PM_{2.5}$ in terms of its toxicological effects in this region has been lacking. With the exception of our own study [45], previous studies in the Midwestern US region have primarily focused on the contribution of various emission sources to $PM_{2.5}$ mass, in both urban and rural areas such as St. Louis, MO [46], Chicago, IL [47], Bondville, IL [48,49], Detroit, MI [47,48,50], Indianapolis, IN [48], and five cities in Iowa (i.e. Cedar Rapids, Des Moines, Davenport, Montgomery and Van Buren) [51]. However, it is important to note that the contribution of emission sources to $PM_{2.5}$ mass do not necessarily correspond with their contribution to the health effects. Huang et al. [52] investigated sources of $PM_{2.5}$ in Georgia (US) and their associations with emergency department (ED) visits for three respiratory diseases (i.e., asthma, pneumonia, and acute upper respiratory infections). Strong correlations were observed for several anthropogenic sources, including suspended dusts, metals, and natural gas, with all respiratory outcomes, while these sources together accounted for less than 15 % of total $PM_{2.5}$ mass. Pennington et al. [53] estimated the associations between $PM_{2.5}$ concentrations of various sources and cardiorespiratory emergency department (ED) visits, and observed strong correlations between respiratory ED visits and certain sources including biomass burning and secondary organic carbon, both of which were again minor contributors to $PM_{2.5}$ mass (< 20 %). These findings pointed out the disparity of emission sources to mass and health impact of $PM_{2.5}$ and thus called for shifting the focus from mass to other more health-relevant properties of $PM_{2.5}$. To somewhat address this concern, our previous study [45] conducted source apportionment analysis on cellular ROS generation from ambient $PM_{2.5}$ in the midwestern region of US. A large number of $PM_{2.5}$ samples (N = 241) were collected from five sites including both urban and rural locations and analyzed for chemical composition, including carbonaceous species, inorganic ions and water-soluble trace elements, and cellular ROS in rat alveolar macrophages (NR8383). The cellular ROS levels were largely attributed to two emission sources – secondary organic aerosols in urban areas and agricultural emissions in rural areas, both of which contributed minorly to the bulk mass of $PM_{2.5}$. While macrophage ROS generation could be an important pathway for assessing the cellular toxicity, it could miss other pathways for oxidative stress occurring in the human body that could be captured by some of the chemical OP assays. This could become even more important in the context of Midwest US, which is rather an understudied region in terms of $PM_{2.5}$ health effects, and particularly OP measurements.

In this study, we present a comprehensive source apportionment analysis for several acellular OP endpoints, i.e., OP^{AA}, OP^{GSH}, $OP^{OH\text{-}SLF}$, OP^{DTT}, and $OP^{OH\text{-}DTT}$ of water-soluble ambient $PM_{2.5}$ in the Midwest US. The same set of ambient $PM_{2.5}$ samples as used in Wang et al. [45] were used and analyzed for acellular OP. Note, the water-soluble acellular OP data on these samples was also previously reported in Yu et al. [40] which focused on the spatiotemporal distribution of $PM_{2.5}$ mass and acellular OP in the Midwest US. Our present study incorporates both water-soluble acellular OP data reported in Yu et al. [40] and source apportionment of $PM_{2.5}$ mass reported in Wang et al. [45], while presenting new investigation of the spatiotemporal trends of $PM_{2.5}$ chemical composition as well as the associations of acellular OP endpoints with chemical composition and emission sources of $PM_{2.5}$. To identify the chemical species sensitive to each acellular OP endpoint, we conducted a univariate regression analysis between OP and measured chemical species of ambient $PM_{2.5}$. Finally, we performed source apportionment on all OP endpoints using positive matrix factorization (PMF), and compared the results with the source apportionment for $PM_{2.5}$ mass. This study provides the first analysis on the emission sources of acellular OP in the Midwestern US and provides insights on the potential sources which might pose a greater impact on the health outcomes than simply contributing to the $PM_{2.5}$ mass.

2. Materials and methods

2.1. Sampling campaign

We collected ambient $PM_{2.5}$ samples using high-volume samplers (Hi-Vol sampler, Thermo Anderson, nominal flow rate = 1.13 m^3/min, equipped with $PM_{2.5}$ impactor) at five sampling sites located in the Midwestern US, which involved three urban sites: Chicago (IL), St. Louis (MO), and Indianapolis (IN), one roadside site in Champaign (IL) and one rural site in Bondville (IL). The detailed sampling methods, including sampling protocols and characteristics of each site, are described in our previous publications [40,45]. Briefly, Chicago (CHI)

and Indianapolis (IND) sites are located in university campuses (Illinois Institute of Technology and Indiana University Purdue University Indianapolis, respectively), and are surrounded by multiple parking garages. St. Louis (STL) site is near an industrial zone, and close (< 1 km) to Mississippi River. All urban sites are close to major highways (within 2 km of the sampling site), e.g., I-90/94 (CHI), I-70 (IND and STL), and I-74 (IND). Champaign (CMP) site is located on the roof of a parking garage, and is adjacent (< 10 m) to a major road (University Ave.) in Champaign city. Bondville (BON) is placed in a rural setting and is relatively far from urban areas (closest city is Champaign, > 5 km). $PM_{2.5}$ were collected on quartz filters (Pall Tissuquartz™, 8" × 10") simultaneously every week from Tuesday 0:00 to Friday 0:00 (duration 72 h) between May 2018 and May 2019 from all the sites, generating 241 samples in total (44 from CHI, 47 from STL, 54 from IND, 51 from CMP, and 45 from BON). Further details of the sampling and weighing protocols are described in the Supplementary Information (SI), Section S1.

2.2. Sample extraction and preparation protocol

All OP assays and most chemical analyses were performed on water extracts of $PM_{2.5}$ samples. For measuring OP and inorganic ions, a few (usually 3–5) punches were cut from filters using metallic punches (16–25 mm diameter) and were immersed into 15–20 mL of de-ionized water (DI). The volume of DI and number of punches were adjusted to achieve ~100 μg of total $PM_{2.5}$ mass per mL. The vials containing filter sections suspended in the DI were sonicated in an ultrasonic water bath for 1 h (Cole-Palmer, Vernon-Hills, IL, US). These suspensions were then filtered through a 0.45 μm PTFE syringe filter to remove all water-insoluble components including the filter fibers. After filtration, 10.5 mL of these extracts were separated and diluted with DI to 15 mL for OP analyses. 3.5 mL aliquots from the remaining extracts were withdrawn, and were diluted to 5 mL for inorganic ion analyses. In the same manner, we extracted several additional punches (1−3) of each filter in DI to prepare for brown carbon (BrC) analysis.

For the measurement of water-soluble organic carbon (WSOC) and metals, 2 punches (each of size 16 mm) were extracted in 5 mL DI, and filtered in the same way as for inorganic ions. Out of this 5 mL, 1.5 mL was used for TOC analysis after being diluted with DI to 25 mL. The diluted extracts were acidified to pH = 2 by adding 20 μL of 70 % nitric acid (HNO_3, molarity = 15.8 M; Avantor Sciences, Radnor, PA, US) to eliminate the interference of inorganic ions in TOC analysis [54]. Another aliquot (2.5 mL) of each 5 mL extract was separated and acidified to pH = 1 (by adding 20 μL of 70 % nitric acid) to prevent the precipitation of metals [55]. This fraction was further diluted to 5 mL before getting analyzed for metals by ICP-MS [45].

2.3. OP assays

The details of OP analyses protocol, including setup of the instrument and its operation, has been previously reported in Yu et al. [56] and Yu et al. [40]. Briefly, we used our semi-automated multi-endpoint reactive oxygen species activity analyzer (SAMERA) for measuring all OP endpoints. In the first step, SAMERA withdraws 3.5 mL of diluted filter extract, and mixes it with 1 mL of 0.5 M potassium phosphate buffer (K-PB, pH = 7.4; treated by Chelex column to remove trace metals prior to use) and 0.5 mL of a surrogate lung fluid (SLF; consisting of 2 mM AA, 1 mM GSH, 3 mM CA, and 1 mM UA. Simultaneously, another 3.5 mL of the PM extract is mixed with 0.5 mL of SLF and 1 mL of K-PB (pH = 7.4) buffered disodium terephthalate (TPT; probe for detecting •OH). At different time intervals, three small aliquots (50 μL) are withdrawn by SAMERA from these mixtures (2 from 1st vial containing sample, K-PB and SLF and 1 from the 2nd vial containing sample, SLF and TPT) and are injected into three separate vials. These aliquots are then diluted by DI and measured for AA, GSH and •OH. 2 mM *o*-phthalaldehyde is added in one of the vials used for measuring GSH.

In the second step, 2.1 mL of the PM extract is mixed with 1.4 mL of DI, 0.5 mL of 1 mM DTT, and 1 mL of 50 mM TPT (prepared in K-PB; pH = 7.4). At different time intervals, two small aliquots (50 μL) are withdrawn and dispensed into two separate vials. DI is added to both vials for measuring DTT and •OH. 500 μL of 0.2 mM 5,5'-dithiobis(2-nitrobenzoic acid) (DTNB) is added to 1st vial to capture residual DTT. Since the concentrations of $PM_{2.5}$ were controlled at 100 μg/mL during the extraction process, the concentrations of $PM_{2.5}$ in RVs for SLF-based (i.e., OP^{AA}, OP^{GSH} and $OP^{OH\text{-}SLF}$) and DTT-based (i.e., OP^{DTT} and $OP^{OH\text{-}DTT}$) endpoints were 50 μg/mL and 30 μg/mL, respectively. After calibration, the slopes of the change in concentration for these measured species, i.e., AA, GSH, DTT, and •OH, are calculated as the depletion (for AA, GSH, and DTT) and generation (for •OH) rates for respective OP endpoints, i.e., OP^{AA}, OP^{GSH}, OP^{DTT}, $OP^{OH\text{-}SLF}$, and $OP^{OH\text{-}DTT}$. The system was cleaned with DI after each step to avoid any carryover of the reagents or samples.

After correcting OP with field blank levels, the OP values were normalized using equivalent volume of the extracted $PM_{2.5}$ sample, as per the following equations:

$$OP_{sample} = OP_{sample,raw} - OP_{blank}$$

$$OP_{sample}v = \frac{\dot{m}_{sample}}{c_{sample}} OP_{sample}$$

where: $OP_{sample,raw}$ and OP_{blank} represent OP values of the sample and the field blank, respectively; $\dot{m}_{sample}$ denotes the mass concentration of $PM_{2.5}$ in ambient air (μg/m^3), and c_{sample} is the concentrations of $PM_{2.5}$ in RVs (μg/mL), and $OP_{sample}v$ is the volume (of air) normalized OP value of the sample.

2.4. Chemical analysis

Water-soluble elements (Ba, Li, Al, K, V, Cr, Mn, Ni, Cu, Zn, As, Se, Pb, and Fe) were measured on the diluted extracts by a NexION 300X inductively coupled plasma mass spectrometry (ICP-MS) (PerkinElmer Inc., Waltham, MA, US) equipped with an integrated autosampler. A daily performance check was run every day before using ICP-MS. For preparing the calibration curve of all metals, Multi-element Calibration Standard (PerkinElmer Inc., Waltham, MA, US) was diluted to designated concentrations of all metals (i.e., 0 ppb, 5 ppb, 10 ppb, 20 ppb, 40 ppb and 80 ppb) and analyzed by ICP-MS.

We employed a Dionex ICS-2100 ion chromatography (IC) (Thermo Fisher Scientific, Waltham, MA, US) equipped with Dionex IonPac AG18 IC anion-exchange column to measure sulfate (SO_4^{2-}), nitrate (NO_3^-), and chloride (Cl^-) ions in the water-soluble extracts of collected $PM_{2.5}$ samples. Note, the levels of Cl^- were mostly below the LOD of our IC, therefore we did not report Cl^- here. For the measurement of ammonium (NH_4^+), we adopted the protocol based on Berthelot reaction, as described in Kanda [57]. Briefly, we used 5 mL of the diluted extract of each sample into a vial, and consecutively added 1 mL of 400 g/L trisodium citrate (NaCit), 0.1 mL of 40 g/L *o*-phenylphenol (OPP), and 0.05 mL of 0.8 % sodium hypochlorite (NaClO) to it. Five minutes later, we added 0.1 mL of 0.5 g/L sodium nitroprusside (NaNP) (dissolved in 3 N sodium hydroxide solution) into the mixture, and placed the vial in a water bath at 40 °C for 15 min. OPP reacts with NH_4^+ in the extract under the presence of NaNP, forming a blue indophenolic dye. The concentration of this dye was then determined by measuring absorbance of the mixture at 670 nm using a spectrophotometer (Shimadzu Corporation, Columbia, MD, US). Ammonium sulfate [$(NH_4)_2SO_4$] standard with known concentrations (0 – 80 μmol NH_4^+/L) were analyzed using the same protocol to obtain the calibration curve for NH_4^+ measurement.

EC and OC were analyzed on a 1.0 × 1.0 cm^2 squared punch taken from the $PM_{2.5}$ filter. A Sunset Lab thermal/optical transmittance (TOT) analyzer (Sunset Laboratory Inc., Tigard, OR, US) was employed following the National Institute for Occupational Safety and Health

(NIOSH) method 5040 [58] for measuring both EC and OC. WSOC were measured using a Shimadzu TOC analyzer (Shimadzu Corporation, Columbia, MD, US). Briefly, diluted and acidified $PM_{2.5}$ extracts (see Section 2.2) were added into a glass bottle (prebaked at 550 °C), and organic carbon was then measured based on a catalytic oxidation combustion technique, which oxidizes organic carbon into carbon dioxide (CO_2) and measures produced CO_2. WSOC concentration was determined by calibrating the instrument with OC standards of known concentrations (0 – 5 ppm) before each batch (~20 samples) of TOC analysis. Brown Carbon (BrC) was measured based on a photometric method. Absorbance of the PM extract at 365 nm with a background correction (at 700 nm) was measured using an online spectrophotometer (Ocean Optics Inc., Dunedin, FL) coupled to a liquid waveguide capillary cell (LWCC-3100; World Precision Instruments Inc., Sarasota, FL). The concentration of BrC in ambient air was calculated by the following equation, as derived from Lambert-Beer law [45].

$$Abs_{BrC} = (A_{365nm} - A_{700nm})\frac{C_a}{lC_l}\ln 10$$

where: Abs_{BrC} is the absorption coefficient of BrC at 365 nm (unit: Mm^{-1}, equivalent to ambient concentration of BrC), $A_{365\ nm}$ and $A_{700\ nm}$ are the absorbance of $PM_{2.5}$ extract at 365 nm and 700 nm, respectively, l is the absorbing path length (1 m for this study), and C_a and C_l are the concentrations of $PM_{2.5}$ in ambient air ($\mu g/m^3$) and in water extracts ($\mu g/mL$), respectively.

2.5. Quality Assurance/Quality Control (QA/QC)

We conducted positive and negative control experiments for all OP analyses. We used a field blank filter extract as the negative control for each set (usually ~10) of $PM_{2.5}$ samples. Different compounds were used as positive controls for different endpoints: Cu(II) for OP^{AA} and OP^{GSH}, Fe(II) for $OP^{OH\text{-}SLF}$, phenanthraquinone for OP^{DTT} and 5-hydroxy-1,4-naphthoquinone for $OP^{OH\text{-}DTT}$, and SAMERA was calibrated weekly with these positive controls. The coefficient of variations (CoVs) for positive control experiments were less than 15 % [40], ensuring a good quality assurance for all OP measurement. All analyses for EC and OC contents were duplicated and the standard deviation of each group was ensured below 5 %. For all other chemical analyses, one sample out of each 10 samples was analyzed in triplicate to ensure the stability of all measurements. Further details of QA/QC analyses for various chemical analyses are provided in SI (section S2).

2.6. Statistical analysis

To assess the spatiotemporal variability in all chemical species, we compared their differences among all sites and seasons using one-way analysis of variance (ANOVA) test conducted in MATLAB, and the individual groups (i.e., between different sites or seasons) were compared in pair by Fisher's least significant difference (LSD) post-hoc test. The differences were considered as significant and highly significant when $p < 0.05$ and $p < 0.01$, respectively. Univariate linear regressions between OP and the concentrations of all chemical species of $PM_{2.5}$ samples were conducted, and Pearson's correlation coefficient (r) were calculated. Correlations were characterized as moderate when $0.30 \leq r < 0.60$, and strong when $r \geq 0.60$.

2.7. Source apportionment analysis

We used a positive matrix factorization (PMF) tool (EPA PMF 5.0) for the source apportionment analysis. PMF model decomposes the profile matrix of chemical species and other source-dependent properties of collected samples into multiple factors with the species profile and contribution to all samples, and reduces the objective function Q to derive an optimum solution to the potential matrices of input data [59]. Q is calculated with the following equation:

$$Q = \sum_{i=1}^{n}\sum_{j=1}^{m}\left(\frac{x_{ij} - \sum_{k=1}^{p} g_{ik}f_{kj}}{u_{ij}}\right)^2$$

where: x_{ij} is the concentration of species j in sample #i, g_{ik} is the contribution of source k to sample #i, f_{kj} is the concentration of species j in source k, and u_{ij} is the uncertainty for each x_{ij}.

We included all chemical species discussed in Section 2.4 as the input variables for source apportionment analysis. The uncertainties for each species were estimated by propagating the uncertainties at each step during the entire analysis process, including sampling and weighing (derived from the $PM_{2.5}$ mass data; 2 – 5 %), extraction (assumed 5 %, not applicable to OC and EC), and analytical uncertainties. Analytical uncertainties were determined by analyzing the positive control (for OP endpoints), commercialized standards (multi-ion anion IC standard solution for inorganic anions, standard solution of ammonium sulfate for ammonium ion, TOC calibration standard for WSOC, and multi-element calibration standard for water-soluble metals) or punches taken multiple times ($N > 6$) from the same filter sample (for EC, OC, and BrC) and calculating the standard deviation from these measurements. Values lower than LOD were replaced by half of LOD, and their corresponding uncertainties were set as 5/6 of LOD. Missing values were replaced by the species median with their corresponding uncertainties as 4 times of the species median [46]. The species with a low signal-to-noise ratio ($S/N < 3$) were identified as weak species in PMF, and their uncertainties were tripled to account for lower confidence in their estimation.

OP normalized by the volume of air sampled (OP_v for all endpoints) and $PM_{2.5}$ mass were apportioned separately for each site. There are two approaches to source appointment analysis of OP: the first is to include OP as an input variable in a receptor model [45,60–63], and the 2nd is to conduct source apportionment of $PM_{2.5}$ mass followed by multiple linear regression for assigning OP to each source [60,64-66]. Although, both of these approaches have their own advantages and disadvantages as discussed in Puthussery et al. [62], method 1 is more effective to capture the sources which are contributing negligibly to $PM_{2.5}$ mass but significantly to OP_v. Given this is the 1st study investigating the sources of acellular OP endpoints in the Midwest US, we chose method 1 to minimize the chances of missing an important source of OP_v. Thus, OP_v was set as the total variable and categorized as a "weak" species in each independent PMF run.

We removed the data for the samples collected during Independence Day period (July 3–5, 2018) for source apportionment due to significant effect of the episodic event of firework emissions on multiple chemical species (e.g., Ba and K) and OP endpoints as reported in Yu et al. [56]. We ran the model multiple times ($N = 20$) for the base run with a seed number of 15. Four to nine factors were tested for obtaining optimal number of factors with highest goodness-of-fit parameter [i.e., Q (robust)] and reasonable factor profiles. G-space plots were obtained to check the correlations among individual factors. Factors with Pearson's correlation coefficients less than 0.4 in these plots were interpreted as distinct, ensuring that our results are free from collinearity.

3. Results and discussion

3.1. $PM_{2.5}$ physicochemical characteristics

3.1.1. Mass balance

The spatiotemporal distribution of $PM_{2.5}$ mass in the Midwestern US is reported in Yu et al. [40]. Briefly, the $PM_{2.5}$ concentrations ranged from 2.0 – 21.7 $\mu g/m^3$ (11.3 ± 3.7 $\mu g/m^3$, median: 11.0 $\mu g/m^3$). Compared to the short-term air quality guidelines suggested by WHO (15 $\mu g/m^3$, 24 h averaged $PM_{2.5}$), approximately 18.3 % of our samples exceeded this threshold, with highest exceedance rate (38.3 %) at the

industrial site STL and lowest (2.2 %) at the rural site BON. Overall, $PM_{2.5}$ mass was homogeneous both seasonally and spatially across the Midwest US. The distribution of $PM_{2.5}$ mass is known to be influenced by various meteorological factors that vary seasonally. For example, the higher mixing layer height during summer may facilitate aerosol dispersion [67], while a lower relative humidity during colder seasons reduces hygroscopic growth of the particles [68]. These meteorological factors may affect the mass concentration of ground-level $PM_{2.5}$, leading to a rather homogeneous distribution of $PM_{2.5}$ concentrations in this region.

We also conducted a mass balance by comparing the reconstituted $PM_{2.5}$ mass concentration from measured chemical species [i.e., inorganic ions, bulk organic matter (OM), EC, and water-soluble elements], with the measured $PM_{2.5}$ mass obtained by weighing the filters (Fig. 1). The reconstituted $PM_{2.5}$ mass concentration was calculated by the following equation:

$$c_m(PM_{2.5})_{rec} = c_m(OM) + c_m(EC) + c_m(SO_4) + c_m(NO_3) + c_m(NH_4) + \sum c_m(\text{elements})$$

where: $c_m(PM_{2.5})_{rec}$ denotes the reconstituted $PM_{2.5}$ mass concentration, and c_m denotes the mass concentration of each species, the unit for all concentrations is μg/m^3. C_m(OM) is calculated as 1.6 times OC for urban sites (i.e. CHI, STL, IND and CMP) and 2.1 times OC for non-urban sites (i.e. BON) [69].

Overall, an excellent correlation was observed between reconstituted and measured $PM_{2.5}$ mass (R^2 = 0.96 – 0.98), while the former accounted for 53 – 64 % of the measured mass. Note, the elements measured by ICP-MS did not include any water-insoluble components. Previous studies have observed a substantial fraction of various metals, e.g., Cu, Fe, and Zn, existing as a part of organic complexes [36,70], which are probably insoluble in water. Roper et al. [71] have reported a higher concentration of Ca, K, and Mg in methanol extracts than water extracts for a set of $PM_{2.5}$ samples collected in Sacramento, CA, indicating their complexation with water-insoluble (and possibly methanol-soluble) organic compounds. Furthermore, silicate salts – an important water-insoluble chemical component in $PM_{2.5}$ in the Midwestern US region [47,51,72], were not measured in our study. All these insoluble components can probably explain the remaining fraction of unaccounted $PM_{2.5}$ mass. Nevertheless, this does not affect the main focus of our study, which is the source apportionment of OP, as OP was also measured on the water-soluble fraction of $PM_{2.5}$. Among the measured chemical species, OM accounted for the highest proportion of measured $PM_{2.5}$ mass (28.4 – 34.7 %, averaged by sites), followed by inorganic ions (16.7 – 27.3 %), EC (1.6 – 4.4 %), and water-soluble elements had the least fraction (0.9 – 1.5 %). These levels of chemical components measured in our study are comparable to the typical ranges reported in other studies conducted in the US urban environments, such as at Los Angeles [73], Baton Rouge [74], Atlanta [75], and New York [76]. The average fraction of $PM_{2.5}$ chemical components at five sites are shown in Fig. 2, and the ambient concentration of these species for all samples are shown in SI (Fig. S1).

3.1.2. *Carbonaceous species*

The seasonally-averaged concentrations of carbonaceous species, including EC, OC, WSOC, and BrC are shown in Fig. 3. The temporal (seasonal) and spatial (among different sites) variabilities of the chemical species as determined by one-way ANOVA test are listed in Tables S1 and S2, respectively. EC levels at all sites ranged from 0.05 – 1.4 μg/m^3 and accounted for 0.7 – 9.7 % (average: 3.1 ± 1.5 %, median: 2.8 %) of the $PM_{2.5}$ mass. We observed strong spatial variation in EC concentration among five sites, with much higher EC level in larger cities (CHI, IND and STL) than the roadside and rural sites in a smaller city (i.e., Champaign). The highest EC concentration occurred at STL in all seasons ($p < 0.01$), except in winter when CHI exhibited the highest EC level. BON, as the most remote site away from urban emissions, had the

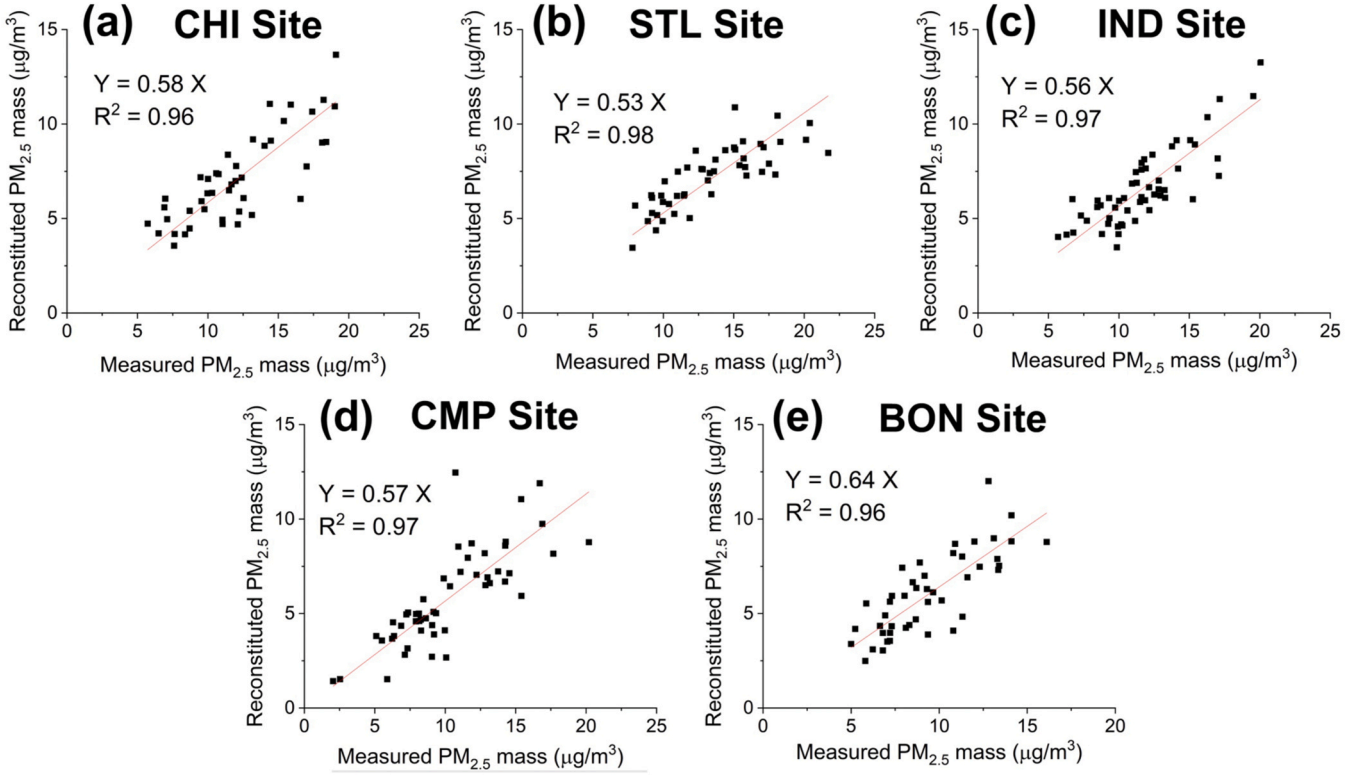

Fig. 1. Orthogonal regression of measured $PM_{2.5}$ mass concentration (X axis) with reconstituted $PM_{2.5}$ mass concentration (by summing measured chemical components; Y axis) for the samples collected at (a) Chicago, IL (CHI); (b) St. Louis, MO (STL); (c) Indianapolis, IN (IND); (d) Champaign, IL (CMP); and (e) Bondville, IL (BON).

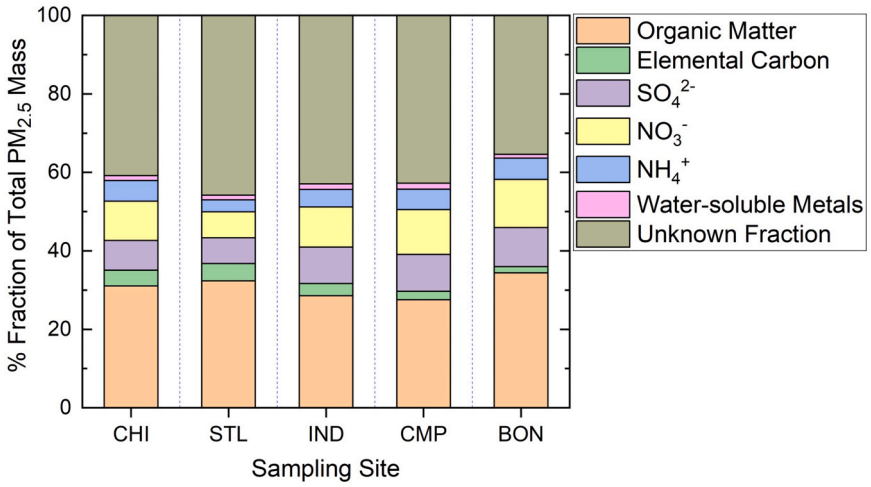

Fig. 2. Average mass fractions of major $PM_{2.5}$ chemical components measured at five sampling sites in the Midwest US: Chicago, IL (CHI); St. Louis, MO (STL); Indianapolis, IN (IND); Champaign, IL (CMP); Bondville, IL (BON).

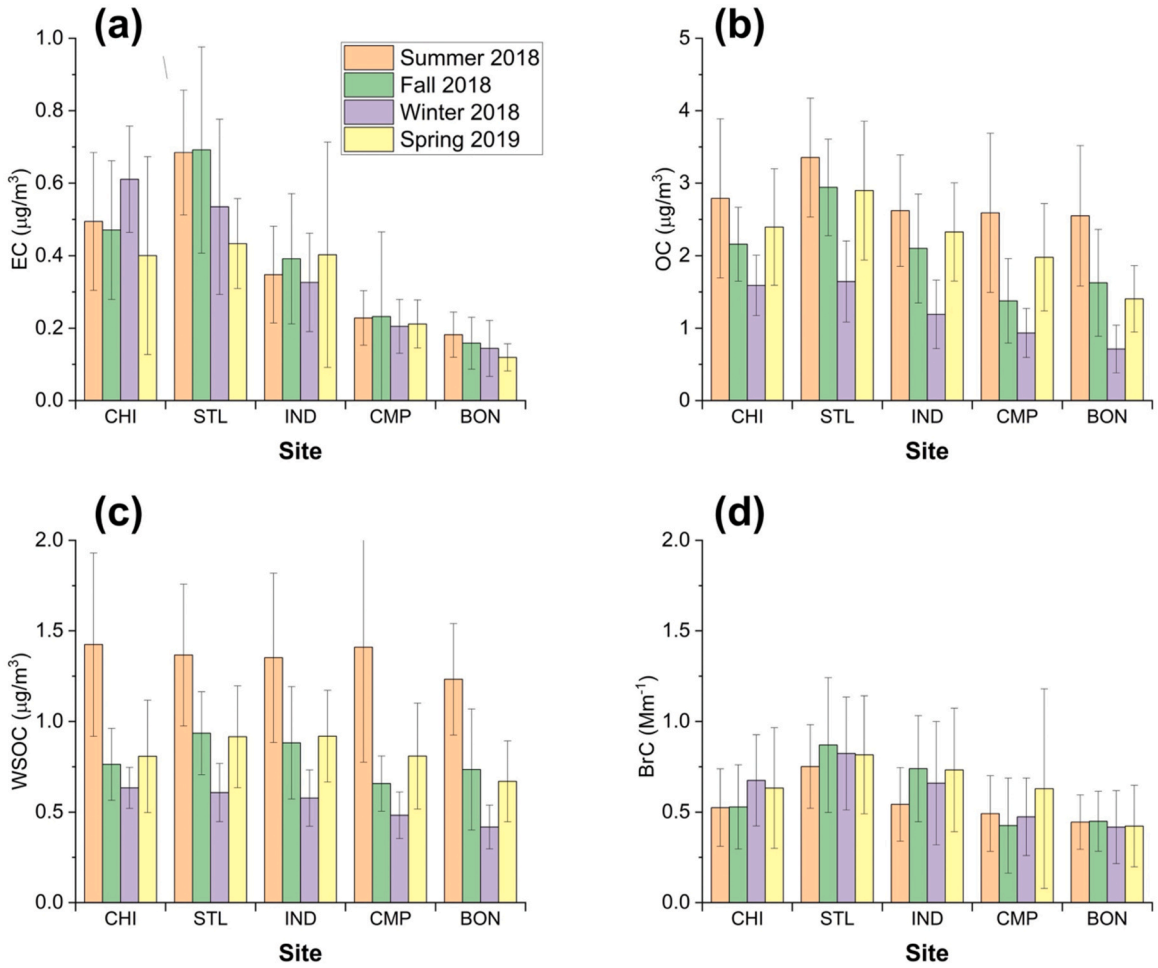

Fig. 3. Seasonal averages of the ambient concentrations of carbonaceous species in ambient $PM_{2.5}$: (a) EC; (b) OC; (c) WSOC; and (d) BrC at different sampling sites in the Midwest US: Chicago, IL (CHI); St. Louis, MO (STL); Indianapolis, IN (IND); Champaign, IL (CMP); Bondville, IL (BON).

lowest EC level across all seasons. There was not much temporal variation in the EC levels at any of the sites except at STL, which showed slightly higher levels in summer and fall ($p < 0.05$). This localized increase might be associated with industrial activities and coal combustion, which are generally more prevalent during warmer seasons, as further corroborated by the findings in Lee et al. [46], showing elevated levels of at least three industrial activities (zinc smelting, lead smelting, and copper production) during both summer and fall.

OC were in the range of 0.3 – 5.4 μg/m^3, and accounted for 4.5 – 37.9 % (average: 18.7 ± 7.4 %, median: 19.0 %) of fine particulate

mass; correspondingly, OM contribution was 7.7 – 78.3 % (average: 31.4 ± 12.7 %, median: 32.1 %). Different from EC, OC showed substantial seasonal variation at all sites, with highest OC levels in summer, followed by spring or fall, and lowest in winter ($p < 0.01$). This seasonal trend might be attributed to the enhanced formation of secondary organic aerosols (SOA) facilitated by increased sunlight during warmer months. Spatially, OC was highest at STL ($p < 0.01$). Other than that, it showed marginal difference between large (CHI and IND) and small (CMP and BON) city sites ($p > 0.05$). WSOC showed identical temporal trend as OC, with highest levels in summer and lowest in winter ($p < 0.01$). Compared to OC, the spatial distribution of WSOC was more homogeneous among different sites. We found an excellent correlation between WSOC and OC at all five sites ($r = 0.87 – 0.94$; Table S3), indicating similar sources for both. On average, the fraction of WSOC accounted for 45.7 ± 12.3 % of OC in $PM_{2.5}$, with highest at BON (53.5 %) and lowest at STL (36.9 %). Different from other carbonaceous species, BrC showed limited variations in both spatial and temporal trends. Spatially, BrC showed highest levels at STL and lowest at BON ($p < 0.01$).

3.1.3. Inorganic ions

The seasonally-averaged concentrations of major inorganic ions, including sulfate (SO_4^{2-}), nitrate (NO_3^-), and ammonium (NH_4^+), are provided in Fig. 4. These inorganic ions in total accounted for 2.7 – 80.4 % (average: 23.1 ± 13.1 %, median: 19.9 %) of $PM_{2.5}$ mass. The levels of SO_4^{2-} ranged from 0.1 – 3.2 μg/m^3 and was spatially uniform. Seasonally, higher SO_4^{2-} levels were generally observed in springtime at CHI, CMP and BON ($p < 0.01$). SO_4^{2-} is produced through photochemical oxidation from sulfur dioxide (SO_2) to sulfuric acid (H_2SO_4); therefore, more intensive sunlight in springtime is expected to promote the production of secondary sulfate aerosols [77].

In contrast, the temporal trends of NO_3^- and NH_4^+ were very different from SO_4^{2-}. Both of these inorganic species showed similar temporal pattern, with peaks in winter at all the sites, followed by fall or spring, and were lowest during summer ($p < 0.01$ at most sites). A strong correlation between NO_3^- and NH_4^+ was observed at all the sites ($r = 0.69 – 0.88$), indicating ammonium nitrate (NH_4NO_3) as the predominant species for these ions in most of our $PM_{2.5}$ samples. This seasonal variability of NO_3^- and NH_4^+ was consistent with the national trend in US [78, 79], resulting from more favorable conditions for partitioning of secondary NH_4NO_3 to aerosol phase in winter, due to lower temperature and shallow boundary layer [51]. Spatially, both of these ions showed a homogeneous distribution throughout the year ($p > 0.05$).

3.1.4. Water-soluble elements

The seasonally-averaged concentrations of water-soluble elements at all the sites are shown in Fig. 5. These water-soluble elements accounted for the smallest fraction (0.4 – 18.9 %; average: 1.2 ± 1.6 %, median: 0.9 %) of total $PM_{2.5}$, with strong variations among seasons and sites. Temporally, most elements, including Cu, Fe, Mn, Al, V, Cr, Ni, Se, and Pb, showed strong seasonal variability ($p < 0.05$ in most cases) with highest levels in summer at most sites (except for V at STL, which peaked in fall), while the differences were less significant among other three seasons. These elements are abundant in the earth crust and their higher summer levels might result from more prominent resuspension of fugitive dust during summer [80]. In addition to the crustal source, a variety of anthropogenic activities also significantly contribute to the emissions of these elements. Cu, Fe, and Pb are predominantly associated with

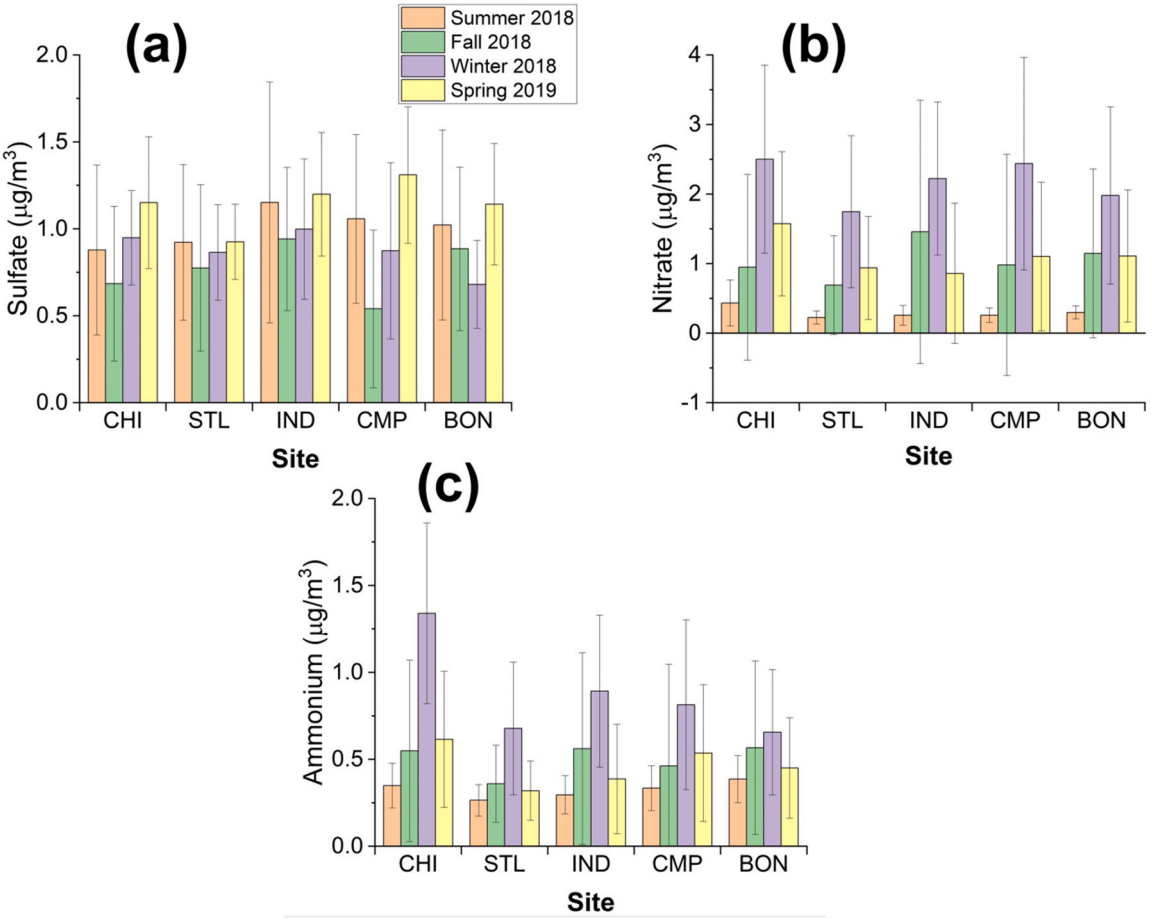

Fig. 4. Seasonal averages of the ambient concentrations of inorganic ions in ambient $PM_{2.5}$: (a) Sulfate; (b) Nitrate; and (c) Ammonium, at different sampling sites in the Midwest US: Chicago, IL (CHI); St. Louis, MO (STL); Indianapolis, IN (IND); Champaign, IL (CMP); Bondville, IL (BON).

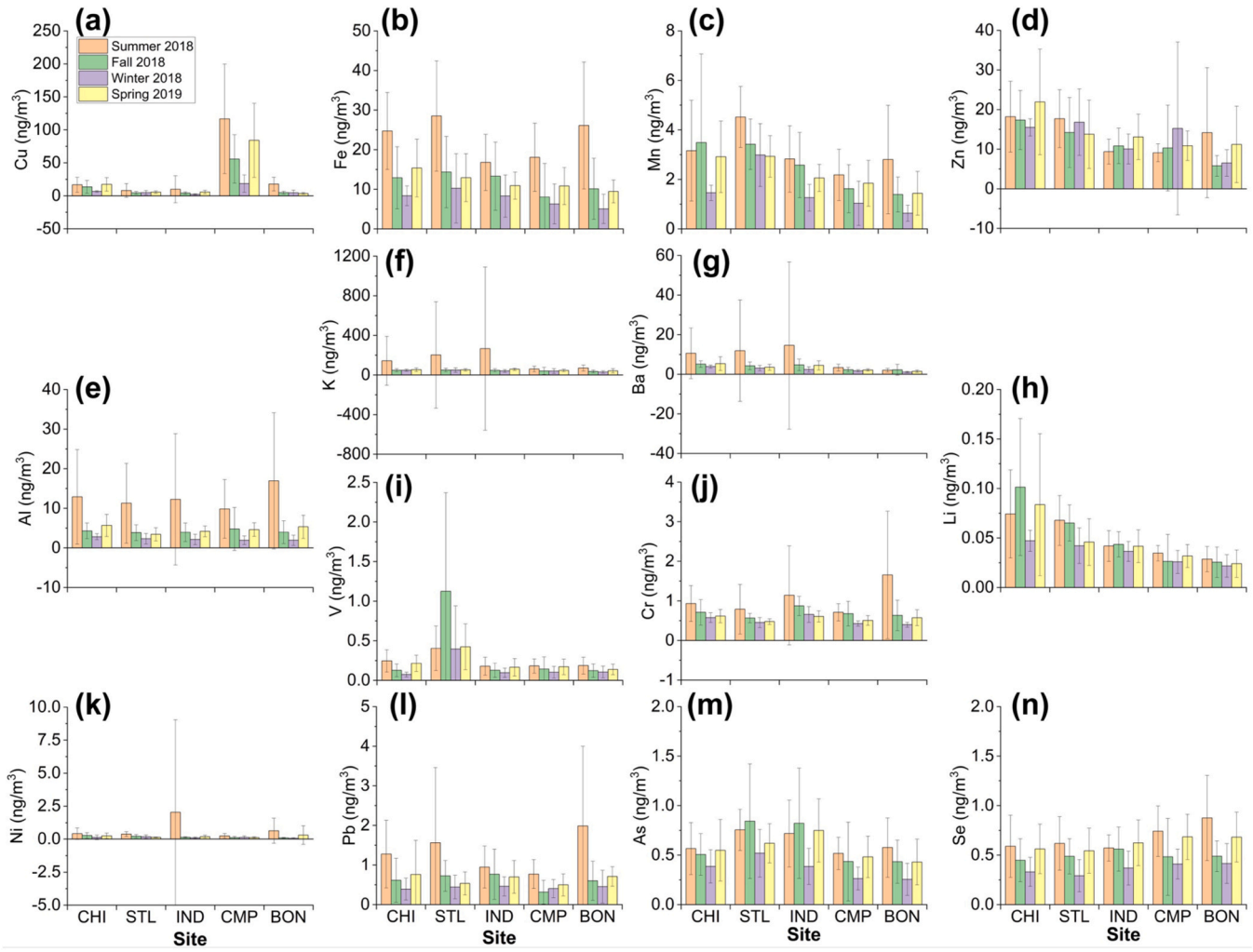

Fig. 5. Seasonal averages of the ambient concentrations of water-soluble elements in ambient $PM_{2.5}$: (a) Cu; (b) Fe; (c) Mn; (d) Zn; (e) Al; (f) K; (g) Ba; (h) Li; (i) V; (j) Cr; (k) Ni; (l) Pb; (m) As; and (n) Se, at different sampling sites in the Midwest US: Chicago, IL (CHI); St. Louis, MO (STL); Indianapolis, IN (IND); Champaign, IL (CMP); Bondville, IL (BON).

vehicular emissions from brake and tire wear as well as from combustion engines [81-83]. Cr, Mn, and Fe have been identified in emissions from industrial activities related to steel-manufacturing and other metal-related industries [84,85]. V and Ni, characterized as important tracers for heavy fuel oil use, are typically linked with shipping and petroleum refinery operations [86,87]. Additionally, Se is associated with various agricultural and industrial activities [88,89]. Other elements, which included Zn, K, Ba, As, and Li, showed marginal seasonal variations ($p > 0.05$). Notably, K and Ba (Fig. 5f and g, respectively) showed a very high standard deviation (329.2 % and 265.6 % of the average, respectively) in summer at three large city sites (i.e., CHI, STL, and IND). This was due to extremely high levels of these species resulting from fireworks emissions during Independence Day celebration (i.e., samples collected from July 3 – 5, 2018) [56]. Vecchi et al. [90] observed a substantial increase in the concentration of K (11 times) and Ba (12 times) in fine particles during a fireworks episode in Milan, Italy. Other studies have also reported a significant elevation of K and Ba levels from fireworks emission during celebratory events like Chinese New Year [91,92], Diwali in India [93,94], and Independence day in US [95,96].

Spatially, it appears that the ambient concentrations of these water-soluble elements were more dominated by the local emissions pertinent to the sites. For example, Cu levels were highest at CMP (2.8 – 23.3 times higher than at other four sites; $p < 0.01$; Fig. 5a) throughout the year, due to its close proximity to a traffic intersection (frequent braking of the vehicles). Note, Cu is one of the major constituents of brake wear emissions [82,97]. High concentration of Cu at CMP site are consistent with our previous studies using the samples collected from the same location ([56,98,99]). CHI was abundant in Zn, Ba, and Li (Fig. 5d, g, and h, respectively). Zn and Ba are important metal tracers of tire wear and brake wear, respectively [81,97]. Due to its proximity to I-57 Expressway, one of the busiest highways in Chicago downtown area, vehicles equipped with diesel and gasoline engines probably contribute significantly to the emission of these species at CHI. Milando et al. [47] also reported substantial contributions from vehicles to Zn (~20 %) at Chicago [47,48]. The elevated levels of Li may be associated with local industrial activities, such as battery manufacturing, metal plating, and recycling facilities [45]. STL, as a site strongly affected by surrounding industries, was enriched in Mn (Fig. 5c) and V (Fig. 5i) throughout the year, Ni (Fig. 5k) during fall, and Fe (Fig. 5b) during summer and winter. Industrial emissions are one of the major sources of Mn [51]. Gatz [100] first reported substantial emissions of Mn and Fe from a large steel mill at Granite City, IL, which is 6.5 km northeast of our STL site. Subsequent source apportionment studies [e.g. Lee and Hopke [72] and Amato and Hopke [101]] have also found a steel processing factor contributing substantially to Mn and Fe at this site. The emissions of V and Ni are reported to be associated with crude oil combustion [87] and ship emissions [55,102]. Ni was also found as a tracer for the diesel exhausts

at this sampling site by Amato and Hopke [101]. Therefore, emissions from surrounding industries, power plants, and ships are probably responsible for the substantially elevated levels of water-soluble metals at STL.

A higher level of Se was observed at BON during summer ($p < 0.05$; Fig. 5n), which is related to the surrounding agricultural activities. As an important supplement of nitrogen-based fertilizers, Se is largely emitted in the atmosphere during fertilizer application period [103,104]. Other water-soluble elements including Al, K, As, and Pb, which are abundant in fugitive dust, showed relatively homogeneous spatial distribution (Fig. 5e,f,l,m) in the Midwest US.

3.2. Correlation between OP and PM composition

To identify the species contributing to OP, we performed a correlation analysis between different OP endpoints and the measured chemical species by individual sites. Pearson's r for univariate linear regression between OP and chemical species for all the seasons combined (i.e., whole year) are listed in Table 1, while those separated by different seasons (summer, fall, winter, and spring) are shown in Table S4 in SI.

3.2.1. Correlations with carbonaceous species

OC and WSOC consistently showed significant correlations with various OP endpoints. Both OC and WSOC were moderately-to-strongly correlated with $OP^{GSH}v$, $OP^{OH\text{-}SLF}v$ and $OP^{DTT}v$ ($r = 0.33 – 0.73$) at CHI, CMP and BON. As reported in numerous studies, OC has shown activities in DTT assay [105,106], cellular GSH/GSSG assay [107], the generation of •OH in SLF [108] and in AA [109]. At STL, OC was moderately correlated with both •OH generation endpoints (i.e. $OP^{OH\text{-}SLF}v$ and $OP^{OH\text{-}DTT}v$; $r = 0.47 – 0.49$). By contrast, no significant correlation was observed for $OP^{AA}v$ with carbonaceous aerosols at any sites. The contrasting patterns between OP^{DTT} and OP^{AA} in their correlations with OC have been reported in several studies [37,110,111]. For example, Yang et al. [111] reported an excellent correlation of OC with $OP^{DTT}v$ ($r = 0.88 – 0.96$) but a poor correlation with $OP^{AA}v$ ($r < 0.3$), using different types of filters and extraction protocols on the samples collected in Netherlands. Seasonally, correlations of OC with $OP^{GSH}v$ and $OP^{DTT}v$ were stronger during winter at CHI, IND, CMP, and BON ($r = 0.47 – 0.92$) than summer ($r < 0.4$).

EC and BrC were moderately correlated with $OP^{GSH}v$, $OP^{OH\text{-}SLF}v$, and $OP^{DTT}v$ at CHI, CMP, and BON ($r = 0.32 – 0.62$) over the entire sampling duration. Sporadic correlations of these two carbonaceous species with other endpoints were also observed, e.g., $OP^{AA}v$ at IND ($r = 0.42 – 0.50$) and $OP^{OH\text{-}DTT}v$ at STL ($r = 0.47 – 0.61$). Both BrC and EC mainly originate from incomplete combustions like biomass burning and fossil fuel combustion [112,113], which could partially explain their similar correlation trends with OP. The correlations of both of these species with SLF-based endpoints and $OP^{DTT}v$ were stronger ($r > 0.50$ for most cases) in winter, during which we believe that biomass burning was a more dominant source. Note, both EC and BrC were correlated with K (a tracer of biomass burning), which was also correlated with both SLF-based endpoints and $OP^{DTT}v$ ($r = 0.45 – 0.84$ for most cases during winter; SI Table S4). A similar trend of strong correlation between EC, BrC, K and all OP endpoints in fall at IND ($r = 0.44 – 0.89$) might also be related to biomass burning, and is further corroborated with a decent correlation between K and EC ($r = 0.58$) and BrC ($r = 0.72$). Moderate-to-strong correlations of EC and BrC with SLF-based endpoints and $OP^{DTT}v$ were observed in fall and spring at CMP ($r = 0.62 – 0.97$ for EC and 0.41 – 0.75 for BrC); however, these correlations were not accompanied by the correlations of K with these endpoints ($r < 0.40$). Since CMP is adjacent to a busy traffic intersection, these correlations might be caused by vehicular emissions – a prominent feature of the roadside site, which contribute substantially to both EC [114,115] and BrC [116,117].

Table 1
Pearson's r for correlation of water-soluble OPv versus $PM_{2.5}$ chemical components at (a) CHI; (b) STL; (c) IND; (d) CMP; and (e) BON. Correlations with $r > 0.60$ are shown in bold.

(a) CHI	$OP^{AA}v$	$OP^{GSH}v$	$OP^{OH\text{-}SLF}v$	$OP^{DTT}v$	$OP^{OH\text{-}DTT}v$
EC	0.10	0.32*	0.41*	**0.62****	0.22
OC	-0.05	0.52**	0.56**	0.39*	0.19
WSOC	-0.02	0.37*	**0.71****	0.33*	0.40**
BrC	-0.07	0.59**	0.10	0.55**	0.17
SO_4^{2-}	0.14	**0.67****	0.37*	0.48**	0.08
NO_3^-	0.10	0.34*	-0.30	0.29	0.10
NH_4^+	0.05	0.30	-0.24	0.37*	0.18
Cu	0.15	**0.73****	0.34*	0.23	0.13
Fe	0.03	0.36*	**0.83****	0.34*	0.35*
Mn	0.07	0.20	0.36*	0.29	0.07
Zn	0.09	0.51**	0.27	0.50**	0.27
Al	0.02	0.36*	**0.74***	0.57**	0.19
K	-0.10	0.39*	0.40**	0.47**	0.31*
Ba	0.01	0.36*	0.32	0.14	0.07
Li	-0.01	0.15	0.25	0.31*	0.03
V	-0.01	0.17	0.46**	0.06	0.33*
Cr	0.02	0.33*	0.55**	0.30	0.19
Ni	-0.05	0.20	0.36*	0.10	0.24
Pb	-0.04	0.23	**0.63****	0.17	0.28
As	-0.01	0.41**	0.48**	0.33*	0.22
Se	-0.08	0.39*	0.48**	0.30	0.40**

(b) STL	$OP^{AA}v$	$OP^{GSH}v$	$OP^{OH\text{-}SLF}v$	$OP^{DTT}v$	$OP^{OH\text{-}DTT}v$
EC	0.32	0.18	0.38*	0.42*	0.47**
OC	0.21	0.17	0.47**	0.29	0.47**
WSOC	0.27	0.22	0.53**	0.25	0.49**
BrC	0.08	0.23	0.11	0.32	**0.61****
SO_4^{2-}	-0.18	0.01	0.00	0.01	0.27
NO_3^-	-0.23	0.04	-0.28	-0.05	0.12
NH_4^+	-0.27	-0.12	-0.29	-0.06	0.17
Cu	**0.92****	**0.80****	0.46**	0.59**	0.08
Fe	0.09	-0.04	0.39*	0.12	0.25
Mn	0.12	0.04	0.36*	0.16	0.25
Zn	-0.03	0.16	0.05	0.14	0.52**
Al	**0.86****	**0.72****	0.58**	**0.61****	0.13
K	0.48**	0.31	0.47**	0.38*	**0.61****
Ba	**0.94****	**0.79****	0.51**	**0.60****	0.02
Li	0.21	0.14	0.46**	0.24	0.36*
V	0.11	0.23	0.50**	0.26	0.52**
Cr	**0.92****	**0.71****	0.49**	0.54**	0.03
Ni	0.16	-0.10	0.32	0.07	0.23
Pb	-0.05	0.05	0.11	0.07	0.23
As	0.31	0.15	0.25	0.24	0.23
Se	0.19	0.04	0.12	0.08	0.32*

(c) IND	$OP^{AA}v$	$OP^{GSH}v$	$OP^{OH\text{-}SLF}v$	$OP^{DTT}v$	$OP^{OH\text{-}DTT}v$
EC	0.50**	0.29	0.24	0.38*	0.15
OC	0.41*	0.17	0.30	0.25	0.02
WSOC	0.39*	0.17	0.33*	0.31*	0.05
BrC	0.42*	0.30	0.11	0.34*	0.17
SO_4^{2-}	0.45**	**0.63****	**0.60****	0.46**	-0.02
NO_3^-	-0.04	0.23	0.07	0.32*	0.28*
NH_4^+	-0.10	0.10	0.03	0.23	0.40**
Cu	0.45**	**0.84****	0.57**	0.45**	-0.16
Fe	0.16	0.02	0.38*	0.26	0.27
Mn	0.26	0.30	**0.62****	0.32*	0.16
Zn	0.33*	0.44**	0.29	0.40**	0.11
Al	0.39*	**0.79****	**0.71****	**0.66****	-0.11
K	0.34*	0.59**	0.36*	0.55**	0.30*
Ba	0.41*	**0.82****	0.51**	0.45**	-0.17
Li	0.57**	0.45**	0.49**	0.35*	0.08
V	-0.01	0.28	0.45**	0.28	-0.01
Cr	0.36*	**0.77****	0.47**	0.35*	-0.19
Ni	-0.09	0.09	-0.11	-0.10	-0.03
Pb	0.16	0.06	0.34*	0.12	0.04
As	0.36*	0.28	0.31*	0.20	-0.07
Se	0.12	0.21	0.27	0.12	0.14
Se	0.19	0.04	0.12	0.08	0.32*

(d) CMP	$OP^{AA}v$	$OP^{GSH}v$	$OP^{OH\text{-}SLF}v$	$OP^{DTT}v$	$OP^{OH\text{-}DTT}v$
EC	0.40**	0.44**	0.34*	0.48**	0.29*
OC	0.38**	0.52**	0.58**	0.42**	0.38**
WSOC	0.31*	0.43**	0.55**	0.34*	0.41**

(continued on next page)

Table 1 (*continued*)

BrC	0.40**	0.56**	0.47**	0.49**	0.37**
SO_4^{2-}	0.23	0.40**	0.24	0.42**	0.25
NO_3^-	-0.09	0.11	-0.23	0.25	0.36*
NH_4^+	-0.08	0.20	-0.14	0.33*	0.47**
Cu	**0.75****	0.59**	**0.69****	**0.67****	-0.06
Fe	0.29	0.26	0.45**	0.40**	0.28
Mn	0.29	0.32*	0.33*	0.33*	0.07
Zn	-0.03	0.09	-0.07	0.06	0.11
Al	0.45**	0.41**	0.55**	0.58**	0.13
K	0.26	0.43**	0.41**	0.52**	0.36
Ba	0.16	0.18	0.56**	0.33*	0.14
Li	0.13	0.43**	0.38**	0.35*	0.28*
V	0.16	0.34*	0.28	0.23	-0.07
Cr	0.21	0.11	0.33*	0.21	0.03
Ni	0.07	0.17	0.24	0.12	0.35*
Pb	0.00	0.28	0.37*	0.14	0.39**
As	0.01	0.30*	0.39**	0.17	0.23
Se	0.05	0.30*	0.37*	0.17	0.30*
(e) BON	$OP^{AA}v$	$OP^{GSH}v$	$OP^{OH\text{-}SLF}v$	$OP^{DTT}v$	$OP^{OH\text{-}DTT}v$
EC	0.16	0.32*	0.50**	0.19	0.35*
OC	0.17	0.52**	0.46**	0.47**	0.29
WSOC	0.37*	**0.61****	**0.73****	0.43**	0.21
BrC	-0.02	0.39**	0.16	0.40**	0.57**
SO_4^{2-}	-0.08	0.12	0.03	0.25	-0.08
NO_3^-	-0.26	-0.14	-0.31	0.12	0.28
NH_4^+	-0.16	-0.04	-0.19	0.22	0.39**
Cu	0.54**	**0.61****	**0.67****	0.52**	0.11
Fe	0.51**	**0.73****	**0.67****	0.51**	0.20
Mn	0.40*	0.56**	**0.64****	0.31*	0.11
Zn	0.21	0.48**	0.46**	0.10	0.19
Al	0.51**	0.57**	**0.60****	0.51**	0.10
K	0.55**	**0.65****	0.59**	0.46**	0.24
Ba	0.27	0.17	0.16	0.16	0.04
Li	0.35*	0.48**	0.40*	0.38**	0.44**
V	0.36*	0.33*	0.17	0.31*	-0.02
Cr	0.38*	0.62**	**0.60****	0.31*	0.18
Ni	0.24	0.43**	0.45**	0.15	-0.01
Pb	0.36*	0.51**	0.56**	0.08	0.21
As	0.19	0.45**	0.50**	0.16	0.25
Se	0.16	0.40**	0.42**	0.10	0.24

* Single asterisks indicate significant ($P < 0.05$) correlations.
** Double asterisks indicate highly significant ($P < 0.01$) correlations.

3.2.2. Correlations with inorganic ions

SO_4^{2-} was moderately-to-strongly correlated with $OP^{GSH}v$, $OP^{OH\text{-}SLF}v$, and $OP^{DTT}v$ at CHI, IND, and CMP (r = 0.37 – 0.67). Seasonally, SO_4^{2-} had moderate-to-strong correlations with SLF-based endpoints and $OP^{DTT}v$ at CHI, IND, and CMP in all seasons except winter (r = 0.45 – 0.90). Since SO_4^{2-} is not a redox-active substance, these correlations might be attributed to secondary organic aerosol, which shares a common formation pathway with inorganic aerosols, i.e. photochemical reactions in warmer and sunny periods [63,77,118,119].

Different from SO_4^{2-}, there was no strong correlation of NO_3^- and NH_4^+ with any OP endpoints in the yearly correlations. Although, we observed some strong seasonal correlations of NO_3^- and NH_4^+ with $OP^{GSH}v$ and $OP^{DTT}v$ during colder seasons, e.g., at CHI (r = 0.46 – 0.75 in fall and spring), STL (r = 0.55 – 0.84 in fall), IND (r = 0.70 – 0.80 in fall), CMP (r = 0.54 – 0.88 in fall and winter) and BON (r = 0.42 – 0.74 in fall and winter). This strong correlation pattern accompanied with the elevated concentration of both NO_3^- and NH_4^+ in colder seasons and might be associated with the partitioning of some redox-active semi-volatile organic compounds into particulate phase at lower temperature [120]. We observed some decent correlations of NO_3^- and NH_4^+ with OC and WSOC during fall and winter at CMP and BON (r = 0.33 – 0.79), which further indicates enhanced partitioning of both secondary organic and inorganic aerosols during colder seasons.

3.2.3. Correlations with water-soluble elements

Several transition metals including Cu, Fe, Mn, and Zn have been frequently linked to OP of $PM_{2.5}$ as reported in numerous studies [37, 110,121–126]. In our study, Cu was almost always correlated with all SLF-based endpoints and $OP^{DTT}v$ at nearly all the sites throughout whole year (r = 0.45 – 0.92). Seasonally, we found moderate-to-strong correlation of Cu with most endpoints in all seasons, including spring at CHI (r = 0.54 – 0.97 for all endpoints), summer, fall and spring at STL (r = 0.57 – 0.94 for most cases), summer and winter at IND (r = 0.50 – 0.99) and all seasons at CMP (r = 0.57 – 0.84 for SLF-based endpoints and $OP^{DTT}v$). This ubiquitous correlation of Cu with OP is consistent with many previous studies using similar endpoints, e.g. OP^{AA} [37,110, 111,127,128], OP^{GSH} [121,127], OP^{DTT} [37,63,111,128] and $OP^{OH\text{-}SLF}$ [129-131]. Cu has the capability to form complexes with both DTT and GSH, which have been shown to actively catalyze the oxidation of remaining fraction (i.e., not complexed with Cu) of DTT and GSH, respectively [132,133]. This complexation can explain the observed correlation of both of these endpoints with the concentration of Cu. Cu can also act as a Fenton reagent, transferring electrons to H_2O_2 and forming •OH [134,135], which is probably reflected in the correlation of Cu with $OP^{OH\text{-}SLF}$. However, the production of •OH by Cu is hindered in the presence of DTT due to the formation of Cu-DTT complex [132]; therefore, we did not see any correlation between Cu and $OP^{OH\text{-}DTT}v$.

We found a moderate-to-strong correlation of Fe with $OP^{OH\text{-}SLF}v$ at all sites in the yearly correlation (r = 0.38 – 0.83). This correlation got further enhanced in certain seasons, i.e., summer, fall and spring at CHI (r = 0.74 – 0.92), fall and winter at IND (r = 0.66 – 0.89), and winter and spring at BON (r = 0.63 – 0.88). The correlations of Fe with other endpoints are more sporadic and were observed only during specific seasons. For example, we observed limited cases of correlations between Fe and $OP^{OH\text{-}DTT}v$ in fall at IND and CMP (r = 0.60 – 0.90). Fe is a known Fenton reagent which catalyzes the reduction of H_2O_2 to •OH [134]. Numerous studies have reported significant associations of Fe with the formation of •OH in SLF [129,131,136–138]. In contrast, our previous study found that Fe alone had a marginal role in $OP^{OH\text{-}DTT}$, but it showed strong activity in presence of HULIS [139]. Therefore, the conditional presence and synergistic interaction of such organic compounds with Fe might be the cause of these limited and sporadic correlations of Fe with $OP^{OH\text{-}DTT}$ in the present study.

Mn was correlated with only $OP^{OH\text{-}SLF}v$ at IND and BON in the yearly correlation (r = 0.62 – 0.64). Since no studies have reported the sensitivity of Mn in $OP^{OH\text{-}SLF}$, this high correlation might be attributed to a common source of Mn and an unidentified OP active species at these two sites. Although, Mn has been shown to be capable of oxidizing DTT in the laboratory studies [105,139], we did not see any significant correlation of Mn with $OP^{DTT}v$ at any site. This could be due to low intrinsic DTT activity of Mn [3.6 nmol/min/μg in 0 – 1 μM Mn^{2+}; 0.3 times of Cu [139]] combined with its relatively lower concentrations at most sites (0.02 – 0.5 times of Cu). Zn was also found to be moderately correlated with $OP^{GSH}v$ and $OP^{DTT}v$ at CHI (r = 0.50 – 0.51), IND (r = 0.40 – 0.44), and $OP^{GSH}v$ at BON (r = 0.48). While we are not aware of any study reporting significant correlation between Zn and OP^{GSH}, Ntziachristos et al. [140] observed strong correlation of Zn with OP^{DTT} in $PM_{0.15}$ (r = 0.93) and moderate correlation in $PM_{2.5}$ (r = 0.52). Two studies have observed DTT loss in presence of Zn, attributing it to the strong binding capability of Zn to DTT [105,141]. Lin and Yu [141] reported a significant DTT depletion within 30 min of the reaction between DTT and Zn, yet considered it to be a false positive result since Zn^{2+} is not redox active. Charrier and Anastasio [105] also observed insignificant DTT consumption rate (0.05 ± 0.06 μM/min) and implied that Zn has no redox catalyzing effect on DTT oxidation. This led us to believe that the sporadic correlations of Zn with these endpoints is coincidental and/or related with a source containing Zn and other redox-active species.

Al, K, V, and Ni were also correlated with OP but only at few sites and during specific seasons, although there is no consistent evidence for the mechanistic role of these elements in any OP endpoints. Al had moderate-to-strong correlations with all SLF-based endpoints and $OP^{DTT}v$ at all the sites (r = 0.36 – 0.86). As a crustal element, Al is

majorly originated from fugitive dust which might be mixed with vehicular emissions containing transition metals [80], some of which (e.g., Cu and Fe) are active in several OP endpoints. A moderate-to-strong correlation of K with SLF-based endpoints and $OP^{DTT}v$ at STL (r = 0.48 – 0.95), IND (r = 0.40 – 0.81), and BON (r = 0.46 – 0.65), as discussed earlier (Section 2.2.1) probably indicates the contribution of biomass burning at these sites. V and Ni were strongly correlated with $OP^{AA}v$, $OP^{OH\text{-}SLF}v$ and $OP^{OH\text{-}DTT}v$ during fall and winter seasons at STL (r = 0.63 – 0.95), which was accompanied by the intercorrelation of these two species (r = 0.91 in fall and 0.59 in winter). Hu et al. (2008) reported a strong correlation among V, Ni, OP^{DTT} and macrophage ROS activity (r = 0.76 – 0.94) at the Long Beach site in California, and attributed this correlation to the emissions of these metals from surrounding ports. St. Louis is the second largest inland port of US, and it serves for one third of the total freight on Mississippi river. Thus, the emissions from ships may contribute to atmospheric V and Ni, resulting into their correlations with OP during colder months. Other water-soluble elements, including Ba, Li, Cr, Pb, As, and Se were also observed to have weak-to-moderate correlations with OP sporadically. These elements had extremely low concentrations (< 5 ng/m^3), and we do not have any evidence for the significant OP activities of any of these elements. Therefore, their correlations are probably associated with their major sources, which will be discussed in the next section.

3.3. Source apportionment of $PM_{2.5}$ mass and OP

The source apportionment was conducted separately with mass and each individual OP endpoint, chosen as the total variable. Overall, we identified 7 sources at urban sites and 6 sources at the rural site, respectively. The common sources among all sites included secondary sulfate, secondary nitrate, SOA, and biomass burning + coal combustion, while there were some local sources, existing only at specific sites, such as agricultural emissions at BON, industrial and shipping emissions at STL, vehicular emissions, parking-related emissions, and road dust at other sites (i.e., CHI, IND, and CMP). The chemical composition profiles with their relative contribution to $PM_{2.5}$ mass at five sites are shown in Fig. S2, while the aggregate contribution of various sources to $PM_{2.5}$ mass and all OP endpoints are shown in Fig. 6. Significant disparities were observed between the contribution of various sources to OP vs. $PM_{2.5}$ mass. The common sources, including three secondary sources (nitrate, sulfate and SOA), combustion-related factors (i.e., biomass burning and coal combustion), and primary vehicular emissions (excluding BON), in total dominated $PM_{2.5}$ mass (>75 %) at all sites, yet their contributions to OP showed different patterns compared to $PM_{2.5}$ mass, which are discussed below.

Three secondary sources together accounted for less than half of total $PM_{2.5}$ at all urban and roadside sites (38.1 – 45.7 %) and approximately two third at the rural site (67.4 %). Secondary nitrate was observed as a major source at all sites (14.4 – 27.4 % of $PM_{2.5}$ mass). As characterized by elevated levels of NO_3^- and NH_4^+, secondary nitrate showed a higher contribution during winter because lower temperatures and longer nights favored heterogeneous hydrolysis of dinitrogen pentoxide (N_2O_5), promoting particle partitioning of ammonium nitrate. Although, secondary nitrate showed some significant contributions to $OP^{DTT}v$ (16.2 – 30.1 %) and $OP^{OH\text{-}DTT}v$ (18.2 – 25.3 %) endpoints, its contribution towards SLF-based endpoints was minimal. NH_4NO_3 does not have any reported redox activity; however, there is a significant presence of BrC in this source, which has been reported to be active in both OP^{DTT} and $OP^{OH\text{-}DTT}$ endpoints [139,142].

Secondary sulfate is characterized by a predominant concentration of SO_4^{2-} with elevated levels during spring and summer due to prevailing photochemical reactions. The contribution of secondary sulfate to $PM_{2.5}$

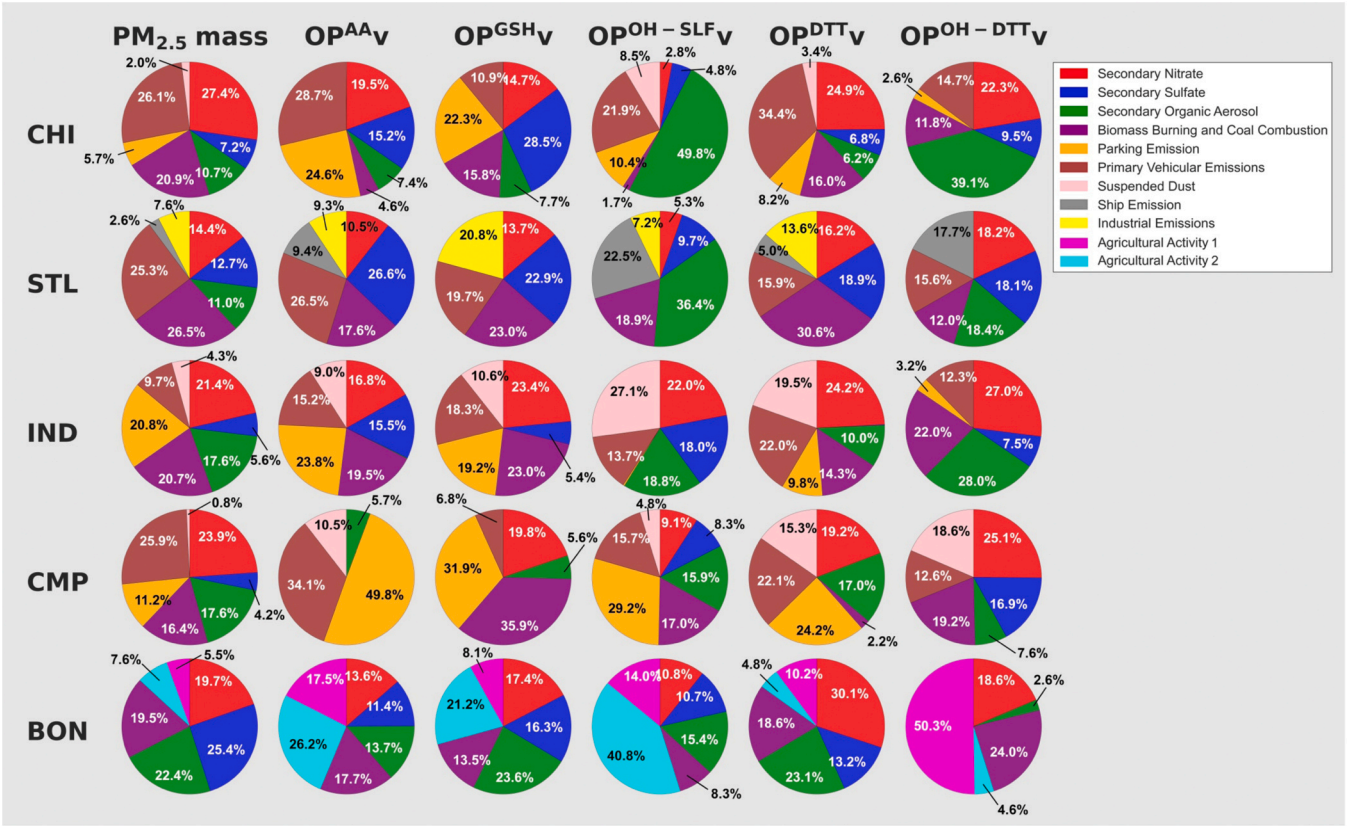

Fig. 6. Annual aggregate contributions of various emission sources to $PM_{2.5}$ mass and five acellular OP endpoints ($OP^{AA}v$, $OP^{GSH}v$, $OP^{OH\text{-}SLF}v$, $OP^{DTT}v$, and $OP^{OH\text{-}DTT}v$) apportioned by PMF at different sampling sites in the Midwest US: Chicago, IL (CHI); St. Louis, MO (STL); Indianapolis, IN (IND); Champaign, IL (CMP); Bondville, IL (BON).

mass was relatively lower at urban sites (i.e., < 15 %). This source showed a strong contribution to $OP^{AA}v$ and $OP^{GSH}v$ at CHI and STL (15.2 – 28.5 %), probably because of enriched WSOC and OC in this factor only at these two sites. Previous $PM_{2.5}$ source apportionment studies conducted in Chicago and St. Louis have also observed a significant presence of OC in the secondary sulfate factor [46,47]. Lee et al. [46] attributed this finding to the heterogeneous formation of organic aerosols under acidic environment during secondary sulfate formation. In contrast, secondary sulfate accounted for 25.4 % of $PM_{2.5}$ mass at the rural site BON but contributed marginally to OP (10.7 – 16.3 %), probably because insignificant OC (< 5 %) present in that factor.

The SOA source, characterized by its high WSOC content and OC/EC ratio, prevailed during summer because of more intensive photochemical activities. This source was also enriched in water-soluble Pb and Fe at all urban sites (i.e., CHI, STL, and IND), which was presumed to result from the complexation of these two transition metals with organic species in the SOA [36]. Although accounting for only 10.7 – 17.6 % of $PM_{2.5}$, SOA contributed substantially to both •OH generation endpoints (15.3 – 49.6 % for $OP^{OH\text{-}SLF}v$ and 18.4 – 39.1 % for $OP^{OH\text{-}DTT}v$) at three urban sites (i.e., CHI, STL, and IND), where elevated fraction of both Fe and Pb were observed. This can be explained by the synergistic reaction between Fe and highly oxygenated organic species (e.g., quinones, HULIS), leading to the formation of •OH in both SLF [70,143,144] and DTT [139,145]. This organic-metallic interaction is further supported by the source profiles at CMP and BON, where SOA factor didn't show any elevated levels of either of these metals and had lower contribution to OP (13.7 – 23.1 %), similar $PM_{2.5}$ mass (17.6 – 22.4 %).

A combustion-related factor was also found at all the sites, with significant levels of K, BrC (markers of biomass burning), As, Se (commonly emitted from coal combustion), EC, and WSOC (probably related with biomass burning). As described in our previous publication [45], we labeled this factor as "biomass burning + coal combustion". This source was observed to increase during summer at all sites except BON, probably due to more intensive coal burning from power plants and the rising frequency of regional wildfires during summer. Previous studies have documented significant impacts of wildfire-emitted $PM_{2.5}$ transported over long distances from California and Canada on the air quality in the Midwest US during wildfire seasons, typically occurring in summer and fall [146,147]. This factor contributed substantially to $PM_{2.5}$ mass (16.4 – 26.5 %) and showed a significant contribution towards certain OP endpoints, including $OP^{GSH}v$ (13.5 – 35.9 %), $OP^{DTT}v$ (14.3 – 30.6 %) and $OP^{OH\text{-}DTT}v$ (11.8 – 24 %). Previous studies have also found significant OP activities of $PM_{2.5}$ emitted from both biomass burning and coal combustion. For example, Mudway et al. [148] reported a substantial GSH depletion rate by the PM collected from dung cake combustion. Dou et al. [149] observed high DTT activities of HULIS extracted from both ambient PM and rice straw burning samples. Yu et al. [66] conducted source apportionment of OP^{DTT} of ambient $PM_{2.5}$ in Beijing and found that coal combustion played the second most important role in OP^{DTT} among all PM sources.

Three vehicular-related factors (primary vehicular emissions, parking-related emissions, and resuspended dust) were apportioned at four urban sites (i.e., CHI, STL, IND, and CMP). Primary vehicular emission source was characterized by its low OC/EC ratio (0.12 – 1.7) and high level of EC and Zn, which are linked with emissions from heavy-duty diesel vehicles (HDDV; e.g., Zn from tire-wear and EC from direct diesel exhausts). This factor was a major source of $PM_{2.5}$ at CHI, STL, and CMP (25.3 – 26.1 %) and a minor source at IND (9.7 %), while having a substantial contribution to $OP^{AA}v$ (15.2 – 34.1 %) and $OP^{DTT}v$ (15.9 – 34.4 %) at all these four sites. These results are consistent with those in Fang et al. [37], which reported a strong contribution of traffic-related emissions to both $OP^{AA}v$ (44 %) and $OP^{DTT}v$ (16 %), as calculated using PMF and chemical mass balance (CMB) models. They attributed this contribution to the co-existence of Cu and OC in this factor, both of which are active in DTT [105,124,139] and AA [124,143,150] assays. Note, the source profile of primary vehicular emissions factor in our study also showed significant amount of both of these species (Cu and OC) at all four sampling sites.

Another vehicular emission factor specifically related to the parking was also identified at CHI, IND, and CMP, with a dominant level of Cu, which mainly originated from brake wear emissions. All these three sites are surrounded by multiple parking garages. Although being a minor source of $PM_{2.5}$ mass at CHI and CMP (5.7 – 11.2 % of $PM_{2.5}$), parking emission contributed significantly to all SLF-based endpoints and $OP^{DTT}v$ (>20 %). From the source profiles (Fig. S2), we could observe that Cu, which is known to play a key role in both SLF and DTT consumption assay (further corroborated by the correlations of Cu with these endpoints; r = 0.45 – 0.92, Table 1), had a substantial presence in this source (46.2 – 71.4 % of Cu) at all three sites. Interestingly, parking emission factor contributed marginally to $OP^{OH\text{-}DTT}v$ (<3 %). Our previous study [139] had reported negligible $OP^{OH\text{-}DTT}$ activity of Cu and a strong antagonistic interaction of Cu with several PM components (e.g., Fe, Mn, quinones, and ambient HULIS) in $OP^{OH\text{-}DTT}$, which could explain the insignificant contribution of parking-related emission factor to this endpoint. Finally, resuspended road dust factor, as featured by enriched crustal elements like Fe, Al, and K, was also found at CHI, IND, and CMP as a minor factor (0.8 – 4.3 % to $PM_{2.5}$ mass). However, this factor contributed significantly to $OP^{OH\text{-}SLF}v$ (4.8 – 27.1 %), $OP^{DTT}v$ (3.4 – 19.5 %) and $OP^{OH\text{-}DTT}v$ (18.6 % at CMP), which might result from the abundance of Fe in this source.

Several other local sources, including an inland-shipping-associated source characterized by elevated levels of V and Ni, an industrial emission source with high concentration of metals (e.g., Al, Zn, and Pb) at STL, and two sources related with agricultural activities at BON, were also identified. These sources generally accounted marginally for $PM_{2.5}$ mass, but their contribution to OP were significant. Ship emissions at STL site accounted for only 2.6 % of $PM_{2.5}$ mass, but contributed more significantly to $OP^{AA}v$ (9.4 %), $OP^{DTT}v$ (5 %), and •OH generation in DTT (17.7 %) and SLF (22.5 %). Dreher et al. [151] used residual oil fly ash (enriched in V and Ni similar to the composition of ship emissions factor) for in vivo lung tests using male Sprague-Dawley rats, and observed a strong association of V and Ni with the formation of ROS in the pulmonary system. Several studies have also reported the contribution of shipping emissions to OP^{AA} and OP^{DTT} at different locations using source apportionment approach [66,152,153]. An industrial emission factor was identified at STL with a broad range of elevated trace metals, e.g., Zn, Cr, Pb, Ni, Cu, and Mn, and metalloids (As and Se). This factor contributed marginally to $PM_{2.5}$ (7.6 %) but significantly to $OP^{GSH}v$ and $OP^{DTT}v$ (13.6 – 20.8 %). Two agriculture-related factors were identified at BON. The first agricultural factor ("agricultural activity 1") featured by elevated levels of As, Zn, Fe, Pb and WSOC is linked with the utilization of fertilizers and herbicides [45] and contributed marginally to $PM_{2.5}$ mass (5.5 %) but substantially to $OP^{OH\text{-}DTT}v$ (50.3 %), probably because of the synergistic effects of Fe and WSOC. The other factor ("agricultural activity 2"), enriched in Al, Ni, Cu, Fe, and Mn, was considered as emissions from sprayer wear [45]. This factor accounted for 7.6 % of $PM_{2.5}$ mass but contributed substantially to all SLF-based endpoints (21.2 – 40.8 %).

Note, although the performance of our PMF model for $PM_{2.5}$ mass was excellent (R^2 = 0.77 – 0.99 for the estimated vs. measured $PM_{2.5}$ mass; Table S5), it was moderate for the OP (R^2 for the estimated and measured OP = 0.43 – 0.82). Many studies have reported non-linear responses of various chemical components to OP endpoints such as OP^{DTT} [105,154,155] and $OP^{OH\text{-}DTT}$ [132,145]. Moreover, both synergistic and antagonistic interactions among PM chemical species have been reported for several OP endpoints such as OP^{AA} [143,150], $OP^{OH\text{-}SLF}$ [70,143,150], OP^{DTT} ([139,142,145,149,156]), and $OP^{OH\text{-}DTT}$ [139,145]. Clearly, these non-linear responses and interaction effects are not effectively captured in the PMF which is based on a linear combination of sources, causing relatively lower performance of PMF for apportioning OP, compared to $PM_{2.5}$ mass. As newer metrics of assessing $PM_{2.5}$ pollution are gaining importance, there is a need to develop

improved statistical tools, such as integrating machine learning algorithms to address the complex relationships between $PM_{2.5}$ chemical composition and source-based toxicities or health effects. Nevertheless, the notable contrast in the contribution of various sources to $PM_{2.5}$ mass and acellular OP is interesting and matches with the findings of our previous study [45] conducted at the same set of sampling sites, which showed a strong disparity in the contribution of different emission sources to $PM_{2.5}$ mass vs. cellular OP using macrophage ROS assay [major sources to macrophage ROS: SOA at urban sites (54–63 %), road dust at CMP (54 %) and agricultural activities at BON (62 %)]. These findings also correspond well with a recent study [64] conducted in Europe using DTT as an OP endpoint, in which the authors found that anthropogenic sources, such as vehicular emissions and anthropogenic SOA had relatively low contribution to PM_{10} mass (< 10 %) but higher contributions to $OP^{DTT}v$ (33 - 88 %). On the contrary, regional secondary inorganic aerosol (SIA) had the largest mass fraction (35 – 60 %) of PM_{10} but showed nearly negligible contribution to $OP^{DTT}v$ at all sites. Collectively, these studies demonstrate the caveat in our current regulatory policies which are focused only on mass concentrations, and highlight the need for a better indicator to represent $PM_{2.5}$ toxicity, to minimize the mortalities associated with $PM_{2.5}$ exposure.

4. Conclusion

Recent research has highlighted disparities in the contributions of various emission sources to $PM_{2.5}$ mass vs. OP across several geographical regions globally, e.g. Europe [60,64,157], China [66, 158–160], and India [161-163]. Our present study builds on the foundational dataset of water-soluble acellular OP and sources of $PM_{2.5}$ mass in the Midwest US discussed in our previous studies [40,45] and investigates the contribution of various $PM_{2.5}$ sources to acellular OP. We observed distinct seasonal trends for different chemical species, with OC, SO_4^{2-}, and most water-soluble metallic species peaking during the summer at most sites, while NO_3^- and NH_4^+ displaying higher levels during winter. Spatially, EC exhibited substantial variation, with higher levels at urban than rural sites. Several water-soluble metals probably associated with local emission sources were also elevated at the specific sites. Generally, the major contributors to $PM_{2.5}$ mass were secondary nitrate (14.4 – 27.4 %), combustion-related (i.e., biomass burning and coal combustion) sources (16.4 – 26.5 %), and primary vehicular emissions (9.7 – 26.1 %), while all of them had relatively lower contributions to most OP endpoints (< 2 – 27.0 %). On the contrary, the contribution of SOA to $PM_{2.5}$ mass was relatively small (10.7 – 17.6 %), while its contribution to $OP^{OH\text{-}SLF}v$ and $OP^{OH\text{-}DTT}v$ was more significant (18.4 – 49.8 %) at large urban city sites (i.e., CHI, STL, and IND) than at small city sites (i.e., CMP and BON, 2.6 – 15.9 %). Compared to these regional sources, local emission sources such as parking-lots traffic and agricultural activities contributed more substantially to OP (up to 50 %) at local city (CMP) and rural (BON) sites, respectively, despite their minor contribution (< 15 %) to $PM_{2.5}$ mass. These results corroborated with the findings from previous OP-source apportionment studies, highlighting the limitations of relying solely on $PM_{2.5}$ mass as an indicator of air pollution, and thus reinforce the need for a shift towards more health-relevant metrics of $PM_{2.5}$ pollution.

We acknowledge that our study had some limitations. First, we did not include the measurement of meteorological parameters in our sampling campaign. Although, our study was focused on quantifying the contribution of various $PM_{2.5}$ sources and their contributions to acellular OP using the non-mechanistic, statistical approach (i.e., PMF), we acknowledge that incorporating these meteorological parameters could have revealed new insights into the modulation of source contributions to OP through meteorological conditions. Second, our study did not incorporate air mass trajectory analysis, which could have also provided further insights into the origins and transport of aerosols from specific sources such as biomass burning and industrial emissions. This could be particularly important for future studies focusing on more localized areas, where integrating this analysis could significantly enhance the understanding of source contributions to $PM_{2.5}$ OP. Nevertheless, our study highlights the need to develop the emission control strategies which not only manage regional sources of $PM_{2.5}$ pollution, but also account for the local sources to minimize the overall health effects from $PM_{2.5}$ pollution.

Environmental implication

Oxidative potential (OP) has been purported as a health relevant metric of ambient $PM_{2.5}$, although ambient air quality standards are based only on $PM_{2.5}$ mass concentrations. Our study investigates the sources of OP of $PM_{2.5}$ across different sites in the midwest region of US. Local sources such as industrial and parking emissions, and agricultural activities, though contributing marginally to $PM_{2.5}$ mass, significantly impact OP. These findings highlight the need to develop the emission control strategies which not only manage regional sources of $PM_{2.5}$ pollution, but also account for the local sources to minimize the overall health effects from $PM_{2.5}$ pollution.

CRediT authorship contribution statement

Joseph V. Puthussery: Writing – review & editing, Resources, Investigation. **Vishal Verma:** Writing – review & editing, Validation, Supervision, Resources, Project administration, Methodology, Funding acquisition, Conceptualization. **Haoran Yu:** Writing – review & editing, Writing – original draft, Visualization, Validation, Resources, Methodology, Investigation, Formal analysis, Data curation, Conceptualization. **Yixiang Wang:** Writing – review & editing, Resources, Investigation, Formal analysis.

Declaration of Competing Interest

The authors declare the following financial interests/personal relationships which may be considered as potential competing interests: Vishal Verma reports financial support was provided by National Science Foundation. If there are other authors, they declare that they have no known competing financial interests or personal relationships that could have appeared to influence the work reported in this paper.

Data availability

Data will be made available on request.

Acknowledgment

This work was supported by the National Science Foundation, USA under Grant No. CBET-1847237.

Appendix A. Supporting information

Supplementary data associated with this article can be found in the online version at doi:10.1016/j.jhazmat.2024.134763.

References

[1] Fiordelisi, A., Piscitelli, P., Trimarco, B., Coscioni, E., Iaccarino, G., Sorriento, D., 2017. The mechanisms of air pollution and particulate matter in cardiovascular diseases. Heart Fail Rev 22 (3), 337–347.
[2] Franklin, M., Zeka, A., Schwartz, J., 2007. Association between PM2. 5 and all-cause and specific-cause mortality in 27 US communities. J Expo Sci Environ Epidemiol 17 (3), 279–287.
[3] Hayes, R.B., Lim, C., Zhang, Y., Cromar, K., Shao, Y., Reynolds, H.R., et al., 2020. PM2. 5 air pollution and cause-specific cardiovascular disease mortality. Int J Epidemiol 49 (1), 25–35.
[4] Pope III, C.A., Burnett, R.T., Thun, M.J., Calle, E.E., Krewski, D., Ito, K., et al., 2002. Lung cancer, cardiopulmonary mortality, and long-term exposure to fine particulate air pollution. JAMA 287 (9), 1132–1141.

[5] Hopke, P.K., Croft, D., Zhang, W., Lin, S., Masiol, M., Squizzato, S., et al., 2019. Changes in the acute response of respiratory diseases to PM2. 5 in New York State from 2005 to 2016. Sci Total Environ 677, 328–339.
[6] Liu, Q., Xu, C., Ji, G., Liu, H., Shao, W., Zhang, C., et al., 2017. Effect of exposure to ambient PM2. 5 pollution on the risk of respiratory tract diseases: a meta-analysis of cohort studies. J Biomed Res 31 (2), 130.
[7] Yan, M., Ge, H., Zhang, L., Chen, X., Yang, X., Liu, F., et al., 2022. Long-term PM2. 5 exposure in association with chronic respiratory diseases morbidity: a cohort study in northern China. Ecotoxicol Environ Saf 244, 114025.
[8] Ailshire, J.A., Crimmins, E.M., 2014. Fine particulate matter air pollution and cognitive function among older US adults. Am J Epidemiol 180 (4), 359–366.
[9] Jung, C.-R., Lin, Y.-T., Hwang, B.-F., 2015. Ozone, particulate matter, and newly diagnosed Alzheimer's disease: a population-based cohort study in Taiwan. J Alzheimer's Dis 44 (2), 573–584.
[10] Zanobetti, A., Dominici, F., Wang, Y., Schwartz, J.D., 2014. A national case-crossover analysis of the short-term effect of PM 2.5 on hospitalizations and mortality in subjects with diabetes and neurological disorders. Environ Health 13 (1), 11.
[11] Hao, Y., Strosnider, H., Balluz, L., Qualters, J.R., 2016. Geographic variation in the association between ambient fine particulate matter (PM2. 5) and term low birth weight in the United States. Environ Health Perspect 124 (2), 250–255.
[12] Li, Z., Tang, Y., Song, X., Lazar, L., Li, Z., Zhao, J., 2019. Impact of ambient PM2. 5 on adverse birth outcome and potential molecular mechanism. Ecotoxicol Environ Saf 169, 248–254.
[13] Twum, C., Zhu, J., Wei, Y., 2016. Maternal exposure to ambient PM2. 5 and term low birthweight in the State of Georgia. Int J Environ Health Res 26 (1), 92–100.
[14] Haberzettl, P., O'Toole, T.E., Bhatnagar, A., Conklin, D.J., 2016. Exposure to fine particulate air pollution causes vascular insulin resistance by inducing pulmonary oxidative stress. Environ Health Perspect 124 (12), 1830–1839.
[15] Liu, C., Xu, X., Bai, Y., Wang, T.-Y., Rao, X., Wang, A., et al., 2014. Air pollution–mediated susceptibility to inflammation and insulin resistance: influence of CCR2 pathways in mice. Environ Health Perspect 122 (1), 17–26.
[16] Mazidi, M., Speakman, J.R., 2017. Ambient particulate air pollution (PM2. 5) is associated with the ratio of type 2 diabetes to obesity. Sci Rep 7 (1), 1–8.
[17] WHO, 2021. WHO global air quality guidelines: particulate matter (PM2. 5 and PM10), ozone, nitrogen dioxide, sulfur dioxide and carbon monoxide. World Health Organization.
[18] Mostofsky, E., Schwartz, J., Coull, B.A., Koutrakis, P., Wellenius, G.A., Suh, H.H., et al., 2012. Modeling the association between particle constituents of air pollution and health outcomes. Am J Epidemiol 176 (4), 317–326.
[19] Bell, M.L., Ebisu, K., Leaderer, B.P., Gent, J.F., Lee, H.J., Koutrakis, P., et al., 2014. Associations of PM2. 5 constituents and sources with hospital admissions: analysis of four counties in Connecticut and Massachusetts (USA) for persons≥ 65 years of age. Environ Health Perspect 122 (2), 138–144.
[20] Bell, M.L., 2012. Assessment of the health impacts of particulate matter characteristics. Res Rep (Health Eff Inst) (161), 5–38.
[21] Cahill, T.A., Barnes, D.E., Spada, N.J., Lawton, J.A., Cahill, T.M., 2011. Very fine and ultrafine metals and ischemic heart disease in the California central valley 1: 2003–2007. Aerosol Sci Technol 45 (9), 1123–1134.
[22] Guo, L.-C., Lv, Z., Ma, W., Xiao, J., Lin, H., He, G., et al., 2022. Contribution of heavy metals in PM2. 5 to cardiovascular disease mortality risk, a case study in Guangzhou, China. Chemosphere 297, 134102.
[23] Masselot, P., Sera, F., Schneider, R., Kan, H., Lavigne, É., Stafoggia, M., et al., 2022. Differential mortality risks associated with PM2. 5 components: a multi-country, multi-city study. Epidemiology 33 (2), 167–175.
[24] Abrams, J.Y., Weber, R.J., Klein, M., Samat, S.E., Chang, H.H., Strickland, M.J., et al., 2017. Associations between ambient fine particulate oxidative potential and cardiorespiratory emergency department visits. Environ Health Perspect 125 (10), 107008. https://doi.org/10.1289/ehp1545.
[25] Bates, J.T., Weber, R.J., Abrams, J., Verma, V., Fang, T., Klein, M., et al., 2015. Reactive oxygen species generation linked to sources of atmospheric particulate matter and cardiorespiratory effects. Environ Sci Technol 49 (22), 13605–13612. https://doi.org/10.1021/acs.est.5b02967.
[26] Weichenthal, S., Lavigne, E., Evans, G., Pollitt, K., Burnett, R.T., 2016. Ambient $PM_{2.5}$ and risk of emergency room visits for myocardial infarction: impact of regional $PM_{2.5}$ oxidative potential: a case-crossover study. Environ Health 15 (1)), 46. https://doi.org/10.1186/s12940-016-0129-9.
[27] Weichenthal, S.A., Lavigne, E., Evans, G.J., Godri Pollitt, K.J., Burnett, R.T., 2016. Fine particulate matter and emergency room visits for respiratory illness. Effect modification by oxidative potential. Am J Respir Crit Care Med 194 (5), 577–586.
[28] He, L., Norris, C., Cui, X., Li, Z., Barkjohn, K.K., Brehmer, C., et al., 2021. Personal exposure to PM2.5 oxidative potential in association with pulmonary pathophysiologic outcomes in children with asthma. Environ Sci Technol 55 (5), 3101–3111. https://doi.org/10.1021/acs.est.0c06114.
[29] Yang, A., Janssen, N.A., Brunekreef, B., Cassee, F.R., Hoek, G., Gehring, U., 2016. Children's respiratory health and oxidative potential of $PM_{2.5}$: the PIAMA birth cohort study. Occup Environ Med 73 (3), 154–160. https://doi.org/10.1136/oemed-2015-103175.
[30] Korsiak, J., Lavigne, E., You, H., Pollitt, K., Kulka, R., Hatzopoulou, M., et al., 2022. Air pollution and pediatric respiratory hospitalizations: effect modification by particle constituents and oxidative potential. Am J Respir Crit Care Med.
[31] Delfino, R.J., Staimer, N., Tjoa, T., Gillen, D.L., Schauer, J.J., Shafer, M.M., 2013. Airway inflammation and oxidative potential of air pollutant particles in a pediatric asthma panel. J Expo Sci Environ Epidemiol 23 (5), 466–473. https://doi.org/10.1038/jes.2013.25.
[32] Maikawa, C.L., Weichenthal, S., Wheeler, A.J., Dobbin, N.A., Smargiassi, A., Evans, G., et al., 2016. Particulate oxidative burden as a predictor of exhaled nitric oxide in children with asthma. Environ Health Perspect 124 (10), 1616. https://doi.org/10.1289/ehp175.
[33] Zhang, X., Staimer, N., Gillen, D.L., Tjoa, T., Schauer, J.J., Shafer, M.M., et al., 2016. Associations of oxidative stress and inflammatory biomarkers with chemically-characterized air pollutant exposures in an elderly cohort. Environ Res 150, 306–319. https://doi.org/10.1016/j.envres.2016.06.019.
[34] Hellack, B., Sugiri, D., Schins, R.P.F., Schikowski, T., Krämer, U., Kuhlbusch, T.A. J., et al., 2017. Land use regression modeling of oxidative potential of fine particles, NO2, PM2.5 mass and association to type two diabetes mellitus. Atmos Environ 171, 181–190. https://doi.org/10.1016/j.atmosenv.2017.10.017.
[35] Strak, M., Janssen, N., Beelen, R., Schmitz, O., Vaartjes, I., Karssenberg, D., et al., 2017. Long-term exposure to particulate matter, NO2 and the oxidative potential of particulates and diabetes prevalence in a large national health survey. Environ Int 108, 228–236.
[36] Wang, Y., Salana, S., Yu, H., Puthussery, J.V., Verma, V., 2022. Relative contributions of iron and organic compounds to and their interaction in the cellular oxidative potential of ambient PM2. 5. Environ Sci Technol Lett.
[37] Fang, T., Verma, V., Bates, J.T., Abrams, J., Klein, M., Strickland, M.J., et al., 2016. Oxidative potential of ambient water-soluble $PM_{2.5}$ in the southeastern United States: contrasts in sources and health associations between ascorbic acid (AA) and dithiothreitol (DTT) assays. Atmos Chem Phys 16 (6), 3865–3879. https://doi.org/10.5194/acp-16-3865-2016.
[38] Yang, A., Wang, M., Eeftens, M., Beelen, R., Dons, E., Leseman, D.L., et al., 2015. Spatial variation and land use regression modeling of the oxidative potential of fine particles. Environ Health Perspect 123 (11), 1187–1192.
[39] Calas, A., Uzu, G., Kelly, F.J., Houdier, S., Martins, J.M., Thomas, F., et al., 2018. Comparison between five acellular oxidative potential measurement assays performed with detailed chemistry on PM 10 samples from the city of Chamonix (France). Atmos Chem Phys 18 (11), 7863–7875.
[40] Yu, H., Puthussery, J.V., Wang, Y., Verma, V., 2021. Spatiotemporal variability in the oxidative potential of ambient fine particulate matter in the Midwestern United States. Atmos Chem Phys 21 (21), 16363–16386.
[41] Dominici, F., McDermott, A., Zeger, S.L., Samet, J.M., 2003. Airborne particulate matter and mortality: timescale effects in four US cities. Am J Epidemiol 157 (12), 1055–1065.
[42] Rosenthal, F.S., Carney, J.P., Olinger, M.L., 2008. Out-of-hospital cardiac arrest and airborne fine particulate matter: a case–crossover analysis of emergency medical services data in Indianapolis, Indiana. Environ Health Perspect 116 (5), 631–636.
[43] Sarnat, S.E., Winquist, A., Schauer, J.J., Turner, J.R., Sarnat, J.A., 2015. Fine particulate matter components and emergency department visits for cardiovascular and respiratory diseases in the St. Louis, Missouri–Illinois, metropolitan area. Environ Health Perspect 123 (5), 437–444.
[44] Zhou, J., Ito, K., Lall, R., Lippmann, M., Thurston, G., 2011. Time-series analysis of mortality effects of fine particulate matter components in Detroit and Seattle. Environ Health Perspect 119 (4), 461–466.
[45] Wang, Y., Puthussery, J.V., Yu, H., Liu, Y., Salana, S., Verma, V., 2021. Sources of cellular oxidative potential of water-soluble fine ambient particulate matter in the midwestern United States. J Hazard Mater, 127777.
[46] Lee, J.H., Hopke, P.K., Turner, J.R., 2006. Source identification of airborne $PM_{2.5}$ at the St. Louis-Midwest Supersite. J Geophys Res Atmos 111 (D10).
[47] Milando, C., Huang, L., Batterman, S., 2016. Trends in $PM_{2.5}$ emissions, concentrations and apportionments in Detroit and Chicago. Atmos Environ 129, 197–209.
[48] Buzcu-Guven, B., Brown, S.G., Frankel, A., Hafner, H.R., Roberts, P.T., 2007. Analysis and apportionment of organic carbon and fine particulate matter sources at multiple sites in the midwestern United States. J Air Waste Manag Assoc 57 (5), 606–619.
[49] Kim, E., Hopke, P.K., Kenski, D.M., Koerber, M., 2005. Sources of fine particles in a rural midwestern U.S. Area. Environ Sci Technol 39 (13), 4953–4960. https://doi.org/10.1021/es0490774.
[50] Gildemeister, A.E., Hopke, P.K., Kim, E., 2007. Sources of fine urban particulate matter in Detroit, MI. Chemosphere 69 (7), 1064–1074. https://doi.org/10.1016/j.chemosphere.2007.04.027.
[51] Kundu, S., Stone, E.A., 2014. Composition and sources of fine particulate matter across urban and rural sites in the Midwestern United States. Environ Sci Process Impacts 16 (6), 1360–1370.
[52] Huang, M., Ivey, C., Hu, Y., Holmes, H.A., Strickland, M.J., 2019. Source apportionment of primary and secondary PM2. 5: associations with pediatric respiratory disease emergency department visits in the US State of Georgia. Environ Int 133, 105167.
[53] Pennington, A.F., Strickland, M.J., Gass, K., Klein, M., Sarnat, S.E., Tolbert, P.E., et al., 2019. Source-apportioned PM2. 5 and cardiorespiratory emergency department visits: accounting for source contribution uncertainty. Epidemiology 30 (6), 789.
[54] Tan, J., Zhang, L., Zhou, X., Duan, J., Li, Y., Hu, J., et al., 2017. Chemical characteristics and source apportionment of PM2.5 in Lanzhou, China. Sci Total Environ 601-602, 1743–1752. https://doi.org/10.1016/j.scitotenv.2017.06.050.
[55] Manousakas, M., Papaefthymiou, H., Eleftheriadis, K., Katsanou, K., 2014. Determination of water-soluble and insoluble elements in PM2.5 by ICP-MS. Sci Total Environ 493, 694–700. https://doi.org/10.1016/j.scitotenv.2014.06.043.
[56] Yu, H., Puthussery, J.V., Verma, V., 2020. A semi-automated multi-endpoint reactive oxygen species activity analyzer (SAMERA) for measuring the oxidative

potential of ambient $PM_{2.5}$ aqueous extracts. Aerosol Sci Technol 54 (3), 304–320.
[57] Kanda, J., 1995. Determination of ammonium in seawater based on the indophenol reaction with o-phenylphenol (OPP). Water Res 29 (12), 2746–2750.
[58] Birch, M., Cary, R., 1996. Elemental carbon-based method for monitoring occupational exposures to particulate diesel exhaust. Aerosol Sci Technol 25 (3), 221–241.
[59] Norris, G., Duvall, R., 2014. EPA Positive Matrix Factorization (PMF) 5.0 fundamentals and user guide. U.S. Environmental Protection Agency. EPA/600/R-14/108.
[60] Cesari, D., Merico, E., Grasso, F.M., Decesari, S., Belosi, F., Manarini, F., et al., 2019. Source apportionment of PM2. 5 and of its oxidative potential in an industrial suburban site in South Italy. Atmosphere 10 (12), 758.
[61] Ma, Y., Cheng, Y., Qiu, X., Cao, G., Fang, Y., Wang, J., et al., 2018. Sources and oxidative potential of water-soluble humic-like substances (HULIS WS) in fine particulate matter (PM 2.5) in Beijing. Atmos Chem Phys 18 (8), 5607–5617.
[62] Puthussery, J.V., Dave, J., Shukla, A., Gaddamidi, S., Singh, A., Vats, P., et al., 2022. Effect of biomass burning, diwali fireworks, and polluted fog events on the oxidative potential of fine ambient particulate matter in Delhi, India. Environ Sci Technol 56 (20), 14605–14616. https://doi.org/10.1021/acs.est.2c02730.
[63] Verma, V., Fang, T., Guo, H., King, L., Bates, J., Peltier, R., et al., 2014. Reactive oxygen species associated with water-soluble $PM_{2.5}$ in the southeastern United States: spatiotemporal trends and source apportionment. Atmos Chem Phys 14 (23), 12915–12930.
[64] Daellenbach, K.R., Uzu, G., Jiang, J., Cassagnes, L.-E., Leni, Z., Vlachou, A., et al., 2020. Sources of particulate-matter air pollution and its oxidative potential in Europe. Nature 587 (7834), 414–419.
[65] Weber, S., Uzu, G., Calas, A., Chevrier, F., Besombes, J.-L., Charron, A., et al., 2018. An apportionment method for the oxidative potential of atmospheric particulate matter sources: application to a one-year study in Chamonix, France. Atmos Chem Phys 18 (13), 9617–9629.
[66] Yu, S., Liu, W., Xu, Y., Yi, K., Zhou, M., Tao, S., et al., 2019. Characteristics and oxidative potential of atmospheric $PM_{2.5}$ in Beijing: Source apportionment and seasonal variation. Sci Total Environ 650, 277–287.
[67] Li, D., Wu, Y., Gross, B., Moshary, F., 2022. Dynamics of mixing layer height and homogeneity from ceilometer-measured aerosol profiles and correlation to ground level PM2. 5 in New York City. Remote Sens 14 (24), 6370.
[68] Shi, J., Hong, J., Ma, N., Luo, Q., He, Y., Xu, H., et al., 2022. Measurement report: on the difference in aerosol hygroscopicity between high and low relative humidity conditions in the North China Plain. Atmos Chem Phys 22 (7), 4599–4613.
[69] Turpin, B.J., Lim, H.-J., 2001. Species contributions to PM2. 5 mass concentrations: revisiting common assumptions for estimating organic mass. Aerosol Sci Technol 35 (1), 602–610.
[70] Wei, J., Yu, H., Wang, Y., Verma, V., 2018. Complexation of iron and copper in ambient particulate matter and its effect on the oxidative potential measured in a surrogate lung fluid. Environ Sci Technol 53 (3), 1661–1671.
[71] Roper, C., Delgado, L.S., Barrett, D., Massey Simonich, S.L., Tanguay, R.L., 2018. PM2. 5 filter extraction methods: implications for chemical and toxicological analyses. Environ Sci Technol 53 (1), 434–442.
[72] Lee, J.H., Hopke, P.K., 2006. Apportioning sources of $PM_{2.5}$ in St. Louis, MO using speciation trends network data. Atmos Environ 40, 360–377.
[73] Sawant, A.A., Na, K., Zhu, X., Cocker III, D.R., 2004. Chemical characterization of outdoor PM2. 5 and gas-phase compounds in Mira Loma, California. Atmos Environ 38 (33), 5517–5528.
[74] Han, F., Kota, S.H., Wang, Y., Zhang, H., 2017. Source apportionment of PM2. 5 in Baton Rouge, Louisiana during 2009–2014. Sci Total Environ 586, 115–126.
[75] Butler, A.J., Andrew, M.S., Russell, A.G., 2003. Daily sampling of PM2. 5 in Atlanta: results of the first year of the assessment of spatial aerosol composition in Atlanta study. J Geophys Res Atmos 108 (D7).
[76] Qin, Y., Kim, E., Hopke, P.K., 2006. The concentrations and sources of PM2. 5 in metropolitan New York City. Atmos Environ 40, 312–332.
[77] Wang, D., Zhou, B., Fu, Q., Zhao, Q., Zhang, Q., Chen, J., et al., 2016. Intense secondary aerosol formation due to strong atmospheric photochemical reactions in summer: observations at a rural site in eastern Yangtze River Delta of China. Sci Total Environ 571, 1454–1466. https://doi.org/10.1016/j.scitotenv.2016.06.212.
[78] Pitchford, M.L., Poirot, R.L., Schichtel, B.A., Malm, W.C., 2009. Characterization of the winter midwestern particulate nitrate bulge. J Air Waste Manag Assoc 59 (9), 1061–1069.
[79] Walker, J., Philip, S., Martin, R., Seinfeld, J., 2012. Simulation of nitrate, sulfate, and ammonium aerosols over the United States. Atmos Chem Phys 12 (22), 11213–11227.
[80] Reff, A., Bhave, P.V., Simon, H., Pace, T.G., Pouliot, G.A., Mobley, J.D., et al., 2009. Emissions inventory of PM2. 5 trace elements across the United States. Environ Sci Technol 43 (15), 5790–5796.
[81] Apeagyei, E., Bank, M.S., Spengler, J.D., 2011. Distribution of heavy metals in road dust along an urban-rural gradient in Massachusetts. Atmos Environ 45 (13), 2310–2323. https://doi.org/10.1016/j.atmosenv.2010.11.015.
[82] Garg, B.D., Cadle, S.H., Mulawa, P.A., Groblicki, P.J., Laroo, C., Parr, G.A., 2000. Brake wear particulate matter emissions. Environ Sci Technol 34 (21), 4463–4469. https://doi.org/10.1021/es001108h.
[83] Hulskotte, J., Denier van der Gon, H., Visschedijk, A., Schaap, M., 2007. Brake wear from vehicles as an important source of diffuse copper pollution. Water Sci Technol 56 (1), 223–231. https://doi.org/10.2166/wst.2007.456.
[84] Hsu, C.-Y., Chi, K.-H., Wu, C.-D., Lin, S.-L., Hsu, W.-C., Tseng, C.-C., et al., 2021. Integrated analysis of source-specific risks for PM2. 5-bound metals in urban, suburban, rural, and industrial areas. Environ Pollut 275, 116652.
[85] Sylvestre, A., Mizzi, A., Mathiot, S., Masson, F., Jaffrezo, J.L., Dron, J., et al., 2017. Comprehensive chemical characterization of industrial PM2. 5 from steel industry activities. Atmos Environ 152, 180–190.
[86] Czech, H., Schnelle-Kreis, J., Streibel, T., Zimmermann, R., 2017. New directions: beyond sulphur, vanadium and nickel–about source apportionment of ship emissions in emission control areas. Atmos Environ 163, 190–191.
[87] Moreno, T., Querol, X., Alastuey, A., de la Rosa, J., de la Campa, A.M.S., Minguillón, M., et al., 2010. Variations in vanadium, nickel and lanthanoid element concentrations in urban air. Sci Total Environ 408 (20), 4569–4579.
[88] He, K.-Q., Yuan, C.-G., Shi, M.-D., Jiang, Y.-H., 2020. Accelerated screening of arsenic and selenium fractions and bioavailability in fly ash by microwave assistance. Ecotoxicol Environ Saf 187, 109820.
[89] Lao, I.R., Feinberg, A., Borduas-Dedekind, N., 2023. Regional sources and sinks of atmospheric particulate selenium in the United States based on seasonality profiles. Environ Sci Technol 57 (19), 7401–7409.
[90] Vecchi, R., Bernardoni, V., Cricchio, D., D'Alessandro, A., Fermo, P., Lucarelli, F., et al., 2008. The impact of fireworks on airborne particles. Atmos Environ 42 (6), 1121–1132.
[91] Li, W., Shi, Z., Yan, C., Yang, L., Dong, C., Wang, W., 2013. Individual metal-bearing particles in a regional haze caused by firecracker and firework emissions. Sci Total Environ 443, 464–469. https://doi.org/10.1016/j.scitotenv.2012.10.109.
[92] Liu, J., Chen, Y., Chao, S., Cao, H., Zhang, A., 2019. Levels and health risks of PM2.5-bound toxic metals from firework/firecracker burning during festival periods in response to management strategies. Ecotoxicol Environ Saf 171, 406–413. https://doi.org/10.1016/j.ecoenv.2018.12.104.
[93] Kulshrestha, U.C., Nageswara Rao, T., Azhaguvel, S., Kulshrestha, M.J., 2004. Emissions and accumulation of metals in the atmosphere due to crackers and sparkles during Diwali festival in India. Atmos Environ 38 (27), 4421–4425. https://doi.org/10.1016/j.atmosenv.2004.05.044.
[94] Pervez, S., Chakrabarty, R.K., Dewangan, S., Watson, J.G., Chow, J.C., Matawle, J.L., 2016. Chemical speciation of aerosols and air quality degradation during the festival of lights (Diwali). Atmos Pollut Res 7 (1), 92–99. https://doi.org/10.1016/j.apr.2015.09.002.
[95] Dickerson, A.S., Benson, A.F., Buckley, B., Chan, E.A., 2017. Concentrations of individual fine particulate matter components in the USA around July 4th. Air Qual Atmos Health 10 (3), 349–358. https://doi.org/10.1007/s11869-016-0433-0.
[96] Kumar, M., Snow, D.D., Li, Y., Shea, P.J., 2019. Perchlorate behavior in the context of black carbon and metal cogeneration following fireworks emission at Oak Lake, Lincoln, Nebraska, USA. Environ Pollut 253, 930–938. https://doi.org/10.1016/j.envpol.2019.07.038.
[97] Grigoratos, T., Martini, G., 2015. Brake wear particle emissions: a review. Environ Sci Pollut Res 22 (4), 2491–2504.
[98] Puthussery, J.V., Zhang, C., Verma, V., 2018. Development and field testing of an online instrument for measuring the real-time oxidative potential of ambient particulate matter based on dithiothreitol assay. Atmos Meas Tech 11 (10), 5767–5780. https://doi.org/10.5194/amt-11-5767-2018.
[99] Wang, Y., Plewa, M.J., Mukherjee, U.K., Verma, V., 2018. Assessing the cytotoxicity of ambient particulate matter (PM) using Chinese hamster ovary (CHO) cells and its relationship with the PM chemical composition and oxidative potential. Atmos Environ 179, 132–141. https://doi.org/10.1016/j.atmosenv.2018.02.025.
[100] Gatz, D.F., 1978. Identification of aerosol sources in the St. Louis area using factor analysis. J Appl Meteorol 17 (5), 600–608. https://doi.org/10.1175/1520-0450(1978)017<0600:ioasit>2.0.co;2.
[101] Amato, F., Hopke, P.K., 2012. Source apportionment of the ambient PM2.5 across St. Louis using constrained positive matrix factorization. Atmos Environ 46, 329–337. https://doi.org/10.1016/j.atmosenv.2011.09.062.
[102] Tao, J., Zhang, L., Cao, J., Zhong, L., Chen, D., Yang, Y., et al., 2017. Source apportionment of PM2. 5 at urban and suburban areas of the Pearl River Delta region, south China-with emphasis on ship emissions. Sci Total Environ 574, 1559–1570.
[103] Chen, L., Yang, F., Xu, J., Hu, Y., Hu, Q., Zhang, Y., et al., 2002. Determination of selenium concentration of rice in China and effect of fertilization of selenite and selenate on selenium content of rice. J Agric Food Chem 50 (18), 5128–5130.
[104] Rady, M.M., Mounzer, O., Alarcón, J., Abdelhamid, M., Howladar, S., 2016. Growth, heavy metal status and yield of salt-stressed wheat (Triticum aestivum L.) plants as affected by the integrated application of bio-, organic and inorganic nitrogen-fertilizers. J Appl Bot Food Qual 89.
[105] Charrier, J., Anastasio, C., 2012. On dithiothreitol (DTT) as a measure of oxidative potential for ambient particles: evidence for the importance of soluble transition metals. Atmos Chem Phys 12 (5), 11317–11350. https://doi.org/10.5194/acp-12-9321-2012.
[106] Verma, V., Rico-Martinez, R., Kotra, N., King, L., Liu, J., Snell, T.W., et al., 2012. Contribution of water-soluble and insoluble components and their hydrophobic/hydrophilic subfractions to the reactive oxygen species-generating potential of fine ambient aerosols. Environ Sci Technol 46 (20), 11384–11392. https://doi.org/10.1021/es302484r.
[107] Li, N., Sioutas, C., Cho, A., Schmitz, D., Misra, C., Sempf, J., et al., 2003. Ultrafine particulate pollutants induce oxidative stress and mitochondrial damage. Environ Health Perspect 111 (4), 455. https://doi.org/10.1289/ehp.6000.

[108] Gonzalez, D.H., Cala, C.K., Peng, Q., Paulson, S.E., 2017. HULIS enhancement of hydroxyl radical formation from Fe (II): kinetics of fulvic acid-Fe (II) complexes in the presence of lung antioxidants. Environ Sci Technol 51 (13), 7676–7685.
[109] Sanchez-Cruz, P., Santos, A., Diaz, S., Alegría, A.E., 2014. Metal-independent reduction of hydrogen peroxide by semiquinones. Chem Res Toxicol 27 (8), 1380–1386.
[110] Janssen, N.A., Yang, A., Strak, M., Steenhof, M., Hellack, B., Gerlofs-Nijland, M.E., et al., 2014. Oxidative potential of particulate matter collected at sites with different source characteristics. Sci Total Environ 472, 572–581. https://doi.org/10.1016/j.scitotenv.2013.11.099.
[111] Yang, A., Jedynska, A., Hellack, B., Kooter, I., Hoek, G., Brunekreef, B., et al., 2014. Measurement of the oxidative potential of $PM_{2.5}$ and its constituents: the effect of extraction solvent and filter type. Atmos Environ 83, 35–42. https://doi.org/10.1016/j.atmosenv.2013.10.049.
[112] Laskin, A., Laskin, J., Nizkorodov, S.A., 2015. Chemistry of atmospheric brown carbon. Chem Rev 115 (10), 4335–4382.
[113] Long, C.M., Nascarella, M.A., Valberg, P.A., 2013. Carbon black vs. black carbon and other airborne materials containing elemental carbon: physical and chemical distinctions. Environ Pollut 181, 271–286.
[114] Chow, J.C., Watson, J.G., Lowenthal, D.H., Antony Chen, L.W., Motallebi, N., 2011. PM2.5 source profiles for black and organic carbon emission inventories. Atmos Environ 45 (31), 5407–5414. https://doi.org/10.1016/j.atmosenv.2011.07.011.
[115] Schauer, J.J., 2003. Evaluation of elemental carbon as a marker for diesel particulate matter. J Expo Sci Environ Epidemiol 13 (6), 443–453.
[116] Hecobian, A., Zhang, X., Zheng, M., Frank, N., Edgerton, E.S., Weber, R.J., 2010. Water-soluble organic aerosol material and the light-absorption characteristics of aqueous extracts measured over the Southeastern United States. Atmos Chem Phys 10 (13).
[117] Liu, J., Bergin, M., Guo, H., King, L., Kotra, N., Edgerton, E., et al., 2013. Size-resolved measurements of brown carbon in water and methanol extracts and estimates of their contribution to ambient fine-particle light absorption. Atmos Chem Phys 13 (24).
[118] Duan, J., Huang, R.-J., Lin, C., Dai, W., Wang, M., Gu, Y., et al., 2019. Distinctions in source regions and formation mechanisms of secondary aerosol in Beijing from summer to winter. Atmos Chem Phys 19 (15), 10319–10334. https://doi.org/10.5194/acp-19-10319-2019.
[119] Yuan, Z.B., Yu, J.Z., Lau, A.K.H., Louie, P.K.K., Fung, J.C.H., 2006. Application of positive matrix factorization in estimating aerosol secondary organic carbon in Hong Kong and its relationship with secondary sulfate. Atmos Chem Phys 6 (1), 25–34. https://doi.org/10.5194/acp-6-25-2006.
[120] Lurmann, F.W., Brown, S.G., McCarthy, M.C., Roberts, P.T., 2006. Processes influencing secondary aerosol formation in the San Joaquin Valley during winter. J Air Waste Manag Assoc 56 (12), 1679–1693.
[121] Godri, K.J., Harrison, R.M., Evans, T., Baker, T., Dunster, C., Mudway, I.S., et al., 2011. Increased oxidative burden associated with traffic component of ambient particulate matter at roadside and urban background schools sites in London. PloS One 6 (7), e21961. https://doi.org/10.1371/journal.pone.0021961.
[122] Moreno, T., Kelly, F.J., Dunster, C., Oliete, A., Martins, V., Reche, C., et al., 2017. Oxidative potential of subway PM2. 5. Atmos Environ 148, 230–238.
[123] Shirmohammadi, F., Wang, D., Hasheminassab, S., Verma, V., Schauer, J.J., Shafer, M.M., et al., 2017. Oxidative potential of on-road fine particulate matter (PM2. 5) measured on major freeways of Los Angeles, CA, and a 10-year comparison with earlier roadside studies. Atmos Environ 148, 102–114.
[124] Visentin, M., Pagnoni, A., Sarti, E., Pietrogrande, M.C., 2016. Urban $PM_{2.5}$ oxidative potential: Importance of chemical species and comparison of two spectrophotometric cell-free assays. Environ Pollut 219, 72–79. https://doi.org/10.1016/j.envpol.2016.09.047.
[125] Weichenthal, S., Shekarrizfard, M., Traub, A., Kulka, R., Al-Rijleh, K., Anowar, S., et al., 2019. Within-city spatial variations in multiple measures of $PM_{2.5}$ oxidative potential in Toronto. Can Environ Sci Technol 53 (5), 2799–2810.
[126] Yang, A., Hellack, B., Leseman, D., Brunekreef, B., Kuhlbusch, T.A., Cassee, F.R., et al., 2015. Temporal and spatial variation of the metal-related oxidative potential of $PM_{2.5}$ and its relation to $PM_{2.5}$ mass and elemental composition. Atmos Environ 102, 62–69.
[127] Künzli, N., Mudway, I.S., Götschi, T., Shi, T., Kelly, F.J., Cook, S., et al., 2006. Comparison of oxidative properties, light absorbance, and total and elemental mass concentration of ambient $PM_{2.5}$ collected at 20 European sites. Environ Health Perspect 114 (5), 684–690. https://doi.org/10.1289/ehp.8584.
[128] Pietrogrande, M.C., Dalpiaz, C., Dell'Anna, R., Lazzeri, P., Manarini, F., Visentin, M., et al., 2018. Chemical composition and oxidative potential of atmospheric coarse particles at an industrial and urban background site in the alpine region of northern Italy. Atmos Environ 191, 340–350. https://doi.org/10.1016/j.atmosenv.2018.08.022.
[129] Charrier, J.G., Anastasio, C., 2011. Impacts of antioxidants on hydroxyl radical production from individual and mixed transition metals in a surrogate lung fluid. Atmos Environ 45 (40), 7555–7562.
[130] DiStefano, E., Eiguren-Fernandez, A., Delfino, R.J., Sioutas, C., Froines, J.R., Cho, A.K., 2009. Determination of metal-based hydroxyl radical generating capacity of ambient and diesel exhaust particles. Inhal Toxicol 21 (9), 731–738.
[131] Vidrio, E., Jung, H., Anastasio, C., 2008. Generation of hydroxyl radicals from dissolved transition metals in surrogate lung fluid solutions. Atmos Environ 42 (18), 4369–4379. https://doi.org/10.1016/j.atmosenv.2008.01.004.
[132] Kachur, A.V., Held, K.D., Koch, C.J., Biaglow, J.E., 1997. Mechanism of production of hydroxyl radicals in the copper-catalyzed oxidation of dithiothreitol. Radiat Res 147 (4), 409–415.
[133] Speisky, H., Gómez, M., Burgos-Bravo, F., López-Alarcón, C., Jullian, C., Olea-Azar, C., et al., 2009. Generation of superoxide radicals by copper–glutathione complexes: redox-consequences associated with their interaction with reduced glutathione. Bioorg Med Chem 17 (5), 1803–1810. https://doi.org/10.1016/j.bmc.2009.01.069.
[134] Goldstein, S., Meyerstein, D., Czapski, G., 1993. The Fenton reagents. Free Radic Biol Med 15 (4), 435–445. https://doi.org/10.1016/0891-5849(93)90043-T.
[135] Held, K.D., Sylvester, F.C., Hopcia, K.L., Biaglow, J.E., 1996. Role of Fenton chemistry in thiol-induced toxicity and apoptosis. Radiat Res 145 (5), 542–553. https://doi.org/10.2307/3579272.
[136] Charrier, J.G., Anastasio, C., 2015. Rates of hydroxyl radical production from transition metals and quinones in a surrogate lung fluid. Environ Sci Technol 49 (15), 9317–9325. https://doi.org/10.1021/acs.est.5b01606.
[137] Ma, S., Ren, K., Liu, X., Chen, L., Li, M., Li, X., et al., 2015. Production of hydroxyl radicals from Fe-containing fine particles in Guangzhou, China. Atmos Environ 123, 72–78. https://doi.org/10.1016/j.atmosenv.2015.10.057.
[138] Shen, H., Anastasio, C., 2011. Formation of hydroxyl radical from San Joaquin Valley particles extracted in a cell-free surrogate lung fluid. Atmos Chem Phys 11 (18), 9671–9682. https://doi.org/10.5194/acp-11-9671-2011.
[139] Yu, H., Wei, J., Cheng, Y., Subedi, K., Verma, V., 2018. Synergistic and antagonistic interactions among the particulate matter components in generating reactive oxygen species based on the dithiothreitol assay. Environ Sci Technol 52 (4), 2261–2270. https://doi.org/10.1021/acs.est.7b04261.
[140] Ntziachristos, L., Froines, J.R., Cho, A.K., Sioutas, C., 2007. Relationship between redox activity and chemical speciation of size-fractionated particulate matter. Part Fibre Toxicol 4 (1), 5.
[141] Lin, P., Yu, J.Z., 2011. Generation of reactive oxygen species mediated by humic-like substances in atmospheric aerosols. Environ Sci Technol 45 (24), 10362–10368.
[142] Zhang, W., Yu, H., Hettiyadura, A.P.S., Verma, V., Laskin, A., 2022. Field evidence for enhanced generation of reactive oxygen species in atmospheric aerosol containing quinoline components. Atmos Environ, 119406.
[143] Lin, M., Yu, J.Z., 2020. Assessment of interactions between transition metals and atmospheric organics: ascorbic acid depletion and hydroxyl radical formation in organic-metal mixtures. Environ Sci Technol 54 (3), 1431–1442. https://doi.org/10.1021/acs.est.9b07478.
[144] Wei, J., Fang, T., Lakey, P.S., Shiraiwa, M., 2021. Iron-facilitated organic radical formation from secondary organic aerosols in surrogate lung fluid. Environ Sci Technol.
[145] Xiong, Q., Yu, H., Wang, R., Wei, J., Verma, V., 2017. Rethinking the dithiothreitol-based particulate matter oxidative potential: measuring dithiothreitol consumption versus reactive oxygen species generation. Environ Sci Technol 51 (11), 6507–6514. https://doi.org/10.1021/acs.est.7b01272.
[146] Burke, M., Driscoll, A., Heft-Neal, S., Xue, J., Burney, J., Wara, M., 2021. The changing risk and burden of wildfire in the United States. Proc Natl Acad Sci 118 (2), e2011048118.
[147] Yang, Z., Demoz, B., Delgado, R., Sullivan, J., Tangborn, A., Lee, P., 2022. Influence of the transported Canadian wildfire smoke on the ozone and particle pollution over the Mid-Atlantic United States. Atmos Environ 273, 118940.
[148] Mudway, I.S., Duggan, S.T., Venkataraman, C., Habib, G., Kelly, F.J., Grigg, J., 2005. Combustion of dried animal dung as biofuel results in the generation of highly redox active fine particulates. Part Fibre Toxicol 2 (1)), 6. https://doi.org/10.1186/1743-8977-2-6.
[149] Dou, J., Lin, P., Kuang, B.-Y., Yu, J.Z., 2015. Reactive oxygen species production mediated by humic-like substances in atmospheric aerosols: Enhancement effects by pyridine, imidazole, and their derivatives. Environ Sci Technol 49 (11), 6457–6465.
[150] Lin, M., Yu, J.Z., 2021. Assessment of oxidative potential by hydrophilic and hydrophobic fractions of water-soluble PM2.5 and their mixture effects. Environ Pollut 275, 116616. https://doi.org/10.1016/j.envpol.2021.116616.
[151] Dreher, K.L., Jaskot, R.H., Lehmann, J.R., Richards, J.H., McGee, J.K., Ghio, A.J., Costa, D.L., 1997. Soluble transition metals mediate residual oil fly ash induced acute lung injury. J Toxicol Environ Health Part A 50 (3), 285–305.
[152] Cheng, Y., Ma, Y., Dong, B., Qiu, X., Hu, D., 2021. Pollutants from primary sources dominate the oxidative potential of water-soluble PM2. 5 in Hong Kong in terms of dithiothreitol (DTT) consumption and hydroxyl radical production. J Hazard Mater 405, 124218.
[153] Perrone, M.R., Bertoli, I., Romano, S., Russo, M., Rispoli, G., Pietrogrande, M.C., 2019. PM2.5 and PM10 oxidative potential at a Central Mediterranean Site: contrasts between dithiothreitol- and ascorbic acid-measured values in relation with particle size and chemical composition. Atmos Environ 210, 143–155. https://doi.org/10.1016/j.atmosenv.2019.04.047.
[154] Calas, A., Uzu, G., Martins, J.M., Voisin, D., Spadini, L., Lacroix, T., et al., 2017. The importance of simulated lung fluid (SLF) extractions for a more relevant evaluation of the oxidative potential of particulate matter. Sci Rep 7 (1), 1–12.
[155] Charrier, J.G., McFall, A.S., Vu, K.K., Baroi, J., Olea, C., Hasson, A., et al., 2016. A bias in the "mass-normalized" DTT response–an effect of non-linear concentration-response curves for copper and manganese. Atmos Environ 144, 325–334. https://doi.org/10.1016/j.atmosenv.2016.08.071.
[156] Wang, S., Ye, J., Soong, R., Wu, B., Yu, L., Simpson, A.J., et al., 2018. Relationship between chemical composition and oxidative potential of secondary organic aerosol from polycyclic aromatic hydrocarbons. Atmos Chem Phys 18 (6), 3987–4003.
[157] Weber, S., Uzu, G., Favez, O., Borlaza, L.J., Calas, A., Salameh, D., et al., 2021. Source apportionment of atmospheric PM 10 oxidative potential: synthesis of 15 year-round urban datasets in France. Atmos Chem Phys Discuss 1–38.

[158] Liu, W., Xu, Y., Liu, W., Liu, Q., Yu, S., Liu, Y., et al., 2018. Oxidative potential of ambient $PM_{2.5}$ in the coastal cities of the Bohai Sea, northern China: seasonal variation and source apportionment. Environ Pollut 236, 514–528.
[159] Wang, Y., Wang, M., Li, S., Sun, H., Mu, Z., Zhang, L., et al., 2020. Study on the oxidation potential of the water-soluble components of ambient PM2. 5 over Xi'an, China: pollution levels, source apportionment and transport pathways. Environ Int 136, 105515.
[160] Zhang, L., Hu, X., Chen, S., Chen, Y., Lian, H.-Z., 2023. Characterization and source apportionment of oxidative potential of ambient PM2. 5 in Nanjing, a megacity of Eastern China. Environ Pollut Bioavailab 35 (1), 2175728.
[161] Bhattu, D., Tripathi, S.N., Bhowmik, H.S., Moschos, V., Lee, C.P., Rauber, M., et al., 2024. Local incomplete combustion emissions define the PM2. 5 oxidative potential in Northern India. Nat Commun 15 (1), 3517.
[162] Gadi, R., Sharma, S.K., Mandal, T.K., 2019. Source apportionment and health risk assessment of organic constituents in fine ambient aerosols (PM2. 5): a complete year study over National Capital Region of India. Chemosphere 221, 583–596.
[163] Singh, A., Patel, A., Satish, R., Tripathi, S., Rastogi, N., 2023. Wintertime oxidative potential of PM2. 5 over a big urban city in the central Indo-Gangetic Plain. Sci Total Environ 905, 167155.